The factorization method for inverse elastic scattering from periodic structures

2013 Inverse Problems 29 115005

(http://iopscience.iop.org/0266-5611/29/11/115005)

Inverse Problems **29** (2013) 115005 (25pp) doi:10.1088/0266-5611/29/11/115005

The factorization method for inverse elastic scattering from periodic structures

Guanghui Hu[1], **Yulong Lu**[2] **and Bo Zhang**[3]

[1] Weierstrass Institute, Mohrenstr. 39, D-10117 Berlin, Germany
[2] Institute of Applied Mathematics, AMSS, Chinese Academy of Sciences, Beijing 100190, People's Republic of China
[3] LSEC and Institute of Applied Mathematics, AMSS, Chinese Academy of Sciences, Beijing 100190, People's Republic of China

E-mail: Guanghui.Hu@wias-berlin.de, luyulong@amss.ac.cn and b.zhang@amt.ac.cn

Received 29 March 2013, in final form 30 July 2013
Published 30 September 2013
Online at stacks.iop.org/IP/29/115005

Abstract
This paper is concerned with the inverse problem of scattering of time-harmonic elastic waves from rigid periodic structures. We establish the factorization method to identify an unknown diffraction grating profile (periodic surface) from knowledge of the scattered compressional or shear waves measured on a line above the periodic surface. Near-field operators are factorized by selecting appropriate incident waves derived from quasi-periodic half-space Green's tensor to the Navier equation. The factorization method gives rise to a uniqueness result for the inverse scattering problem by utilizing only the compressional or shear components of the scattered field corresponding to all quasi-periodic incident plane waves with a common phase-shift. A number of computational examples are provided to show the accuracy of the inversion algorithms, with emphasis placed on comparing reconstructions from the scattered near field and those from its compressional and shear components.

(Some figures may appear in colour only in the online journal)

1. Introduction

The inverse scattering problem of recovering an unknown diffraction grating profile (periodic structure) from the scattered field is of great importance, e.g., in diffractive optics, quality control and design of diffractive elements with prescribed far-field patterns [7, 32]. Consequently, there is a vast literature on the reconstruction of grating interfaces modeled by the Maxwell equations or the two-dimensional Helmholtz equation (see e.g. [1, 5, 6, 15, 18, 19, 21, 28, 30, 33, 34]). The inverse elastic scattering by periodic structures also has a wide field of applications, particularly in geophysics, seismology and nondestructive testing. For instance, identifying fractures in sedimentary rocks can have significant impact on the production of underground gas and liquids by employing controlled explosions. The sedimentary rock under consideration can be regarded as a homogeneous transversely isotropic elastic medium with periodic vertical fractures that can be extended to infinity in one of the horizontal directions. Using an elastic plane wave as an incoming source, we thus obtain an inverse problem of shape identification from knowledge of near-field data measured above the periodic structure; see [29]. Analogous inverse problems also arise from using transient elastic waves to measure the elastic properties or to detect flaws and cracks in concrete structures. Moreover, the problem of elastic pulse transmission and reflection through the earth is fundamental to both the investigation of earthquakes and the utility of seismic waves in search for oil and ore bodies [16, 17].

This paper is concerned with the inverse elastic diffraction problem (IP) of recovering a two-dimensional rigid diffraction grating profile from the scattered near field, which can be regarded as a simple model problem in elasticity. The direct scattering problem (DP) can be formulated as a Dirichlet boundary value problem for the time-harmonic Navier equation in the unbounded domain above the scattering periodic surface. We refer to [3, 4, 11, 12, 14] or section 2 of this paper concerning existence and uniqueness results for the direct scattering problem. We shall establish the factorization method for (IP), generalizing the inversion algorithms in acoustic scattering from bounded obstacles [6, 10, 23, 25] and diffraction gratings [5, 6, 28] to the current situation. The factorization method was first put forward by Kirsch [23] to reconstruct bounded obstacles from the spectral data of the far-field operator. It requires neither computation of direct solutions nor initial guesses and provides a sufficient and necessary condition for precisely characterizing the shape of the unknown scatterers. We refer to [24, 30, 31] for the factorization method applied to inverse electromagnetic scattering from bounded obstacles and diffraction gratings. Schiffer's uniqueness theorem for (IP) was already justified in [2]. It was proved that a smooth diffraction grating surface (C^2) can be uniquely determined from incident pressure waves for one incident angle and an interval of wave numbers. Furthermore, a finite set of wave numbers is enough if *a priori* information about the height of the grating curve is known. This extends the periodic version of Schiffer's theorem by Hettlich and Kirsch (see [19]) to the case of inverse elastic diffraction problems. The application of the Kirsch–Kress optimization scheme to (IP) with one or several incident elastic plane waves can be found in [13].

Compared with the scattering of acoustic waves, the elastic scattering is more complicated in view of the coexistence of compressional (also called longitudinal or dilatational) waves and shear (also called transverse or distortional) waves that propagate at different speeds. We divide our inverse problems into two classes, depending on the phase-shifts of the incident elastic plane waves for a fixed incident angle. For each class, we study the associated inverse problems by utilizing the scattered compressional waves, shear waves or the entire scattered near field. As a corollary, we obtain a uniqueness result using only the information of the scattered compressional or shear waves corresponding to all incident elastic plane waves with a common phase-shift. Such a result is in analogy with the one in [20] for bounded rigid obstacles using only compressional or shear waves.

Inspired by the existing factorization methods for diffraction gratings [5, 28] as well as for bounded obstacle scattering in a half-space [25, chapter 2.6], we choose two admissible sets of incident waves based on the form of the quasi-periodic elastic Green's tensor in a half-plane. Such a Green's tensor is derived from the general (non-quasi-periodic) half-plane Green's function (see [4]) through Poisson's formula. The admissible sets of incident waves enable us to factorize the near-field operators in a standard way. However, it should be pointed out that the incident elastic waves we used are very artificial (see section 3) since they have the same quasi-periodic phase-shift determined by a fixed incident angle and consist of not only downward propagating waves but also upward propagating waves. This is because using only the downward propagating incident waves cannot lead to a desired factorization of the near-field operator which an appropriate range identity can be applied to. On the other hand, it is still an open problem on how to establish the factorization method by using a finite number of plane waves with different incident angles in the range $(-\pi/2, \pi/2)$; see section 3 for more discussion. To apply appropriate range identities, we investigate the properties of the middle operator for small frequencies; see remark 4.12. This differs from the factorization method established in [5, 28], where the role of the positive part of the middle operator is played by a single-layer operator whose kernel is the quasi-periodic fundamental solution to the Helmholtz equation with the wave number $k = i$ or $k = 0$. The injectivity of the middle operator is justified under the assumption that the frequency of the incident waves is not the quasi-periodic Dirichlet eigenvalue of the Lamé operator over a periodic strip.

The paper is organized as follows. In section 2, we formulate the direct and inverse elastic scattering problems for diffraction gratings and collect some solvability results for the direct problem. Section 3 is devoted to describing the half-space quasi-periodic Green's tensor and two admissible sets of incident elastic waves with distinct phase-shifts. In section 4, we provide a theoretical justification of the factorization method, following the spirit of [5, 20]. Numerical experiments are reported in section 5 to test the validity and stability of the factorization method, with an emphasis on comparing reconstructions from utilizing the scattered near field and those from its compressional and shear components.

2. Direct and inverse scattering problems

Let the diffraction grating profile be given by the graph Λ of a C^2-smooth 2π-periodic function f lying above the x_1-axis, i.e., $\Lambda = \{x_2 = f(x_1) > 0, x_1 \in \mathbb{R}\}$. Denote by Ω_Λ the unbounded region above Λ and assume, for simplicity, that Ω_Λ is occupied by a linear isotropic and homogeneous elastic material with mass density 1. Suppose an incident pressure wave (with the incident angle $\theta \in (-\pi/2, \pi/2)$) given by

$$u_p^{\text{in}} = \hat{\theta} \exp(\mathrm{i}k_p x \cdot \hat{\theta}), \quad \hat{\theta} := (\sin\theta, -\cos\theta)^T, \quad x = (x_1, x_2) \in \mathbb{R}^2, \tag{2.1}$$

is incident on Λ from the region above. Here, $k_p := \omega/\sqrt{2\mu + \lambda}$ is the compressional wave number, λ and μ denote the Lamé constants satisfying that $\mu > 0$ and $\lambda + \mu > 0$, $\omega > 0$ is the angular frequency of the harmonic motion and the symbol $(\cdot)^T$ stands for the transpose of a vector in $\mathbb{R}^2$. The shear wave number is defined as $k_s := \omega/\sqrt{\mu}$. The direct problem for incident pressure waves aims to find the scattered field $u^{\text{sc}} \in H^1_{\text{loc}}(\Omega_\Lambda)^2$ such that

$$(\Delta^* + \omega^2)u^{\text{sc}} = 0 \quad \text{in} \quad \Omega_\Lambda, \quad \Delta^* := \mu\Delta + (\lambda + \mu)\,\text{grad div}, \tag{2.2}$$

$$u^{\text{sc}} = -u_p^{\text{in}} \quad \text{on} \quad \Lambda. \tag{2.3}$$

Recall that a function u is called quasi-periodic with the phase-shift α (or α-quasi-periodic) if

$$u(x_1 + 2\pi, x_2) = \exp(2\mathrm{i}\alpha\pi)\, u(x_1, x_2), \quad (x_1, x_2) \in \Omega_\Lambda. \tag{2.4}$$

Obviously, the incident pressure wave u_p^{in} is α-quasi-periodic with $\alpha = k_p \sin\theta$ over the periodic domain Ω_Λ. If the scattered field u^{sc} is also supposed to be quasi-periodic with the same phase-shift as the incident wave, then problem (2.2) admits a unique solution that satisfies the outgoing Rayleigh expansion

$$u^{\text{sc}}(x) = \sum_{n\in\mathbb{Z}} \left\{ A_{p,n} W_{p,n} \begin{pmatrix} \alpha_n \\ \beta_n \end{pmatrix} \mathrm{e}^{\mathrm{i}\alpha_n x_1 + \mathrm{i}\beta_n x_2} + A_{s,n} W_{s,n} \begin{pmatrix} \gamma_n \\ -\alpha_n \end{pmatrix} \mathrm{e}^{\mathrm{i}\alpha_n x_1 + \mathrm{i}\gamma_n x_2} \right\} \tag{2.5}$$

for all x lying above the line $\Gamma_h := \{x_2 = h\}$. Here, h is an arbitrary number satisfying $h \geqslant \Lambda^+ := \max_{(x_1,x_2)\in\Lambda} x_2$, the constants $A_{p,n}, A_{s,n} \in \mathbb{C}$ are called the Rayleigh coefficients, and the weights $W_{p,n}$ and $W_{s,n}$ are defined by

$$W_{p,n} := \begin{cases} 1, & \text{if} \quad |\alpha_n| < k_p, \\ \exp(-\mathrm{i}\beta_n h), & \text{if} \quad |\alpha_n| \geqslant k_p, \end{cases} \qquad W_{s,n} := \begin{cases} 1, & \text{if} \quad |\alpha_n| < k_s, \\ \exp(-\mathrm{i}\gamma_n h), & \text{if} \quad |\alpha_n| \geqslant k_s, \end{cases} \tag{2.6}$$

and

$$\alpha_n := \alpha + n, \qquad \beta_n = \beta_n(\theta) := \begin{cases} \sqrt{k_p^2 - \alpha_n^2} & \text{if} \quad |\alpha_n| \leqslant k_p, \\ \mathrm{i}\sqrt{\alpha_n^2 - k_p^2} & \text{if} \quad |\alpha_n| > k_p. \end{cases} \tag{2.7}$$

The parameter $\gamma_n := \gamma_n(\theta)$ is defined similarly as β_n with k_p replaced by k_s. For uniqueness and existence of solutions to problem (2.2)–(2.5), we refer to [3] where the integral equation method is used for smooth (C^2) grating profiles and to [11, 12] where the variational approach is applied to the case of general Lipschitz graphs in $\mathbb{R}^n$ ($n = 2, 3$). It is recently proved in [14] that such an α-quasi-periodic solution is the unique solution to problem (2.2)–(2.5) in the weighted Sobolev space

$$H^1_\varrho(S_h) := \{u : u = \left(1 + x_1^2\right)^{-\varrho/2} v,\ v \in H^1(S_h)\}, \qquad S_h := \Omega_\Lambda \backslash \{x = (x_1, x_2) : x_2 > h\}$$

for every $h > \Lambda^+$ and $-1 < \varrho < -1/2$. This implies that non-quasi-periodic or other α'-quasi-periodic ($\alpha' \neq k_p \sin\theta$) solutions to problem (2.2)–(2.5) do not exist in the space $H^1_\varrho(S_h)$. These solvability results in periodic structures extend those in acoustics (see [8, 9, 22]) to the case of elasticity. Moreover, they remain valid for a large class of quasi-periodic incident elastic waves as considered in the subsequent sections of this paper, provided the scattering surface is given by the graph of a periodic function. For non-graph grating profiles, the existence of solutions to problem (2.2)–(2.5) can be proved by applying the Fredholm alternative (see [11, 12]).

Since β_n and γ_n are real for at most a finite number of indices $n \in \mathbb{Z}$, only a finite number of plane waves in (2.5) propagate into the far field, with the remaining evanescent waves (or surface waves) decaying exponentially as $x_2 \to +\infty$. The above expansion (2.5) converges uniformly with all derivatives in the half-plane $\{x \in \mathbb{R}^2 : x_2 \geqslant h\}$ for $h > \Lambda^+$ and the Rayleigh coefficients $\{A_{p,n}\}_{n\in\mathbb{Z}}, \{A_{s,n}\}_{n\in\mathbb{Z}} \in \ell^2$. The scattered field can be decomposed into its compressional and shear parts:

$$u^{\mathrm{sc}} = u_p^{\mathrm{sc}} + u_s^{\mathrm{sc}}, \quad u_p^{\mathrm{sc}} := -1/k_p^2 \,\mathrm{grad}\,\mathrm{div}\, u^{\mathrm{sc}}, \quad u_s^{\mathrm{sc}} := 1/k_s^2 \,\overrightarrow{\mathrm{curl}}\,\mathrm{curl}\, u^{\mathrm{sc}},$$

where $\mathrm{curl}\, u := \partial_1 u_2 - \partial_2 u_1$ for a vector function $u = (u_1, u_2)^T$ and $\overrightarrow{\mathrm{curl}}\, w = (\partial_2 w, -\partial_1 w)^T$ for a scalar function w. In particular, the P- and S-waves admit the Rayleigh expansions

$$\begin{aligned} u_p^{\mathrm{sc}} &:= \sum_{n\in\mathbb{Z}} \left[A_{p,n} W_{p,n} (\alpha_n, \beta_n)^T \exp(\mathrm{i}\alpha_n x_1 + \mathrm{i}\beta_n x_2)\right], \\ u_s^{\mathrm{sc}} &:= \sum_{n\in\mathbb{Z}} \left[A_{s,n} W_{s,n} (\gamma_n, -\alpha_n)^T \exp(\mathrm{i}\alpha_n x_1 + \mathrm{i}\gamma_n x_2)\right] \end{aligned} \tag{2.8}$$

for $x_2 > h > \Lambda^+$, respectively, and satisfy the equations

$$(\Delta + k_p^2) u_p^{\mathrm{sc}} = 0, \quad \mathrm{curl}\, u_p^{\mathrm{sc}} = 0, \quad (\Delta + k_s^2) u_s^{\mathrm{sc}} = 0, \quad \mathrm{div}\, u_s^{\mathrm{sc}} = 0 \quad \text{in} \quad \Omega_\Lambda.$$

The uniqueness and existence results for an incident pressure wave can all be extended to the case with an incident shear wave u_s^{in} of the form

$$u_s^{\mathrm{in}} = \hat{\theta}^\perp \exp(\mathrm{i}k_s x \cdot \hat{\theta}), \quad \hat{\theta} := (\sin\theta, -\cos\theta)^\top, \quad \hat{\theta}^\perp := (\cos\theta, \sin\theta)^\top, \tag{2.9}$$

which is $k_s \sin\theta$-quasi-periodic. Note that the phase-shift of the (unique) scattered field corresponding to (2.9) is $\alpha = k_s \sin\theta$, which differs from the case of P-wave incidence given in (2.1).

In this paper, we are interested in the inverse problem of recovering an unknown rigid diffraction grating profile (periodic scattering surface) Λ from the knowledge of the scattered near field measured on Γ_h for some fixed $h > \Lambda^+$. Thus, the line Γ_h denotes our detection or measurement position. We always assume that the unknown grating profile Λ lies between the lines $\Gamma_0 := \{x_2 = 0\}$ and Γ_h for some large $h > 0$. Let $\mathcal{I}_1(\alpha)$ and $\mathcal{I}_2(\alpha)$ be two different admissible sets of elastic waves that are α-quasi-periodic. Given a fixed incident angle $\theta \in (-\pi/2, \pi/2)$, this paper is devoted to studying the following inverse problems $(\mathbf{P}_j)$ and $(\mathbf{S}_j)$, $j = 1, 2, 3$, by using $k_p \sin\theta$-quasi-periodic and $k_s \sin\theta$-quasi-periodic elastic waves.

$(\mathbf{P}_1)$ Reconstruct the diffraction grating profile Λ from the Rayleigh coefficients $A_{p,n}$, $n \in \mathbb{Z}$, of the compressional part u_p^{sc} of the scattered near field on Γ_h corresponding to each incident elastic wave $u^{\mathrm{in}} \in \mathcal{I}_1(\alpha)$ with $\alpha = k_p \sin\theta$.

$(\mathbf{P}_2)$ Reconstruct the diffraction grating profile Λ from the Rayleigh coefficients $A_{s,n}$, $n \in \mathbb{Z}$, of the shear part u_s^{sc} of the scattered near field on Γ_h corresponding to each incident elastic wave $u^{\mathrm{in}} \in \mathcal{I}_2(\alpha)$ with $\alpha = k_p \sin\theta$.

$(\mathbf{P}_3)$ Reconstruct the diffraction grating profile Λ from the Rayleigh coefficients $A_{p,n}, A_{s,n}$, $n \in \mathbb{Z}$, of the scattered near field u^{sc} on Γ_h corresponding to each incident elastic wave $u^{\mathrm{in}} \in \mathcal{I}_1(\alpha) \cup \mathcal{I}_2(\alpha)$ with $\alpha = k_p \sin\theta$.

The inverse problems $(\mathbf{S}_j)$ are formulated similarly as $(\mathbf{P}_j)$ with the quasi-periodicity parameter replaced by $\alpha = k_s \sin\theta$. Our aim is to establish the factorization method for numerically solving the inverse problems $(\mathbf{P}_j)$ and $(\mathbf{S}_j)$ and compare the numerical results by using quasi-periodic incident waves with different phase-shifts and by using different components of the scattered field. The admissible sets $\mathcal{I}_j(\alpha)$ of incident waves will be explicitly defined in the following section.

3. The admissible sets of incident elastic waves

In contrast to the inverse scattering from bounded obstacles, the angle of incidence for diffraction gratings has to be restricted to $(-\pi/2, \pi/2)$ in order to reconstruct the diffraction grating profile from above. However, it does not seem to be suitable to employ incident waves with distinct angles in the range $(-\pi/2, \pi/2)$ since the quasi-periodicity of the scattered field varies with the angle of incidence. In the acoustic case, the authors of [5] suggest using the following set of incident waves having a common phase-shift

$$\left\{ u_n^{\mathrm{in}}(y) := \frac{\mathrm{i}}{4\pi\beta_n}[\mathrm{e}^{\mathrm{i}(\alpha_n y_1 - \beta_n y_2)} - \mathrm{e}^{\mathrm{i}(\alpha_n y_1 + \beta_n y_2)}],\ n \in \mathbb{Z} \right\}, \quad y = (y_1, y_2) \in \mathbb{R}^2, \tag{3.1}$$

where β_n is defined as in (2.7) with k_p replaced by k. In (3.1), it is assumed that $\beta_n \neq 0$ for all $n \in \mathbb{Z}$, that is, the Rayleigh frequencies are excluded. Consequently, the periodic version of the factorization method can be justified by using the single-layer potential whose kernel is the α-quasi-periodic Green's function to the Helmholtz equation $(\Delta + k^2)u = 0$ in a half-plane. Note that each function u_n^{in} in (3.1) satisfies the Dirichlet boundary condition on Γ_0 and consists of both upward and downward wave modes and that using only the downward wave modes cannot lead to a desired factorization of the near-field operator to which an appropriate range identity can be applied. Recall the following α-quasi-periodic Green's function to the

Helmholtz equation $\Delta u + k^2 u = 0$ (see, e.g., [27]):

$$G_k(x,y) = \frac{\mathrm{i}}{4\pi}\sum_{n\in\mathbb{Z}}\frac{1}{\beta_n}\exp(\mathrm{i}\alpha_n(x_1-y_1)+\mathrm{i}\beta_n|x_2-y_2|), \quad x=(x_1,x_2),\ y=(y_1,y_2)\in\mathbb{R}^2$$

with $x-y\neq n(2\pi,0)^T$. Then, the difference $G_k(x,y)-G_k(x,y')$, with $y'=(y_1,y_2)':=(y_1,-y_2)$, is just the α-quasi-periodic Green's function in the half-space $x_2>0$ satisfying the Dirichlet boundary condition on the boundary $x_2=0$. Observe further that the incident wave $u_n^{\mathrm{in}}(y)$ coincides with the conjugate of the nth Rayleigh coefficient of the function $x\to G_k(x,y)-G_k(x,y')$ for $x_2>y_2$. Inspired by these facts in acoustics, we introduce the following two admissible sets of incident elastic waves for $(\mathbf{P}_j)$ and $(\mathbf{S}_j)$, $j=1,2,3$:

$$\mathcal{I}_j(\alpha) := \left\{u_{j,n}^{\mathrm{in}}(y),\ n\in\mathbb{Z}\right\}, \quad j=1,2,$$

where $u_{1,n}^{\mathrm{in}}(y)$ (or $u_{2,n}^{\mathrm{in}}(y)$) is defined as the conjugate of the nth Rayleigh coefficient of the compressional (or shear) part of the function $x\to\Pi_D(x,y)$ (or multiplied by some constant) for $x_2>y_2>0$. Here, $\Pi_D(x,y)$ stands for the α-quasi-periodic half-space Green's tensor to the Navier equation with the Dirichlet boundary condition on Γ_0. The expression of $\Pi_D(x,y)$, which seems unknown by far in the literature, will be derived from the free-space elastic Green's tensor in the remaining part of this section.

We first recall the free-space fundamental solution to the Navier equation (2.2) (see, e.g., [4]):

$$\Gamma(x,y) = \frac{1}{\mu}\Phi_{k_s}(x,y)\,I + \frac{1}{\omega^2}\mathrm{grad}_x\,\mathrm{grad}_x^T[\Phi_{k_s}(x,y)-\Phi_{k_p}(x,y)],$$

where I, Φ_k stand for the 2×2 unit matrix and the free-space fundamental solution to the Helmholtz equation, respectively. Then, the α-quasi-periodic fundamental solution (Green's tensor) to the Navier equation takes the form

$$\Pi(x,y) := \sum_{n\in\mathbb{Z}}\exp(-\mathrm{i}\alpha 2\pi n)\Gamma(x+n(2\pi,0),y), \quad x-y\neq n(2\pi,0), \quad n\in\mathbb{Z}.$$

We refer to [3, section 6] for the convergence analysis of the above series. Similarly to the form of $\Gamma(x,y)$, the tensor $\Pi(x,y)$ can be written as (see [11])

$$\begin{aligned}\Pi(x,y) &= \frac{1}{\mu}G_{k_s}(x,y)I + \frac{1}{\omega^2}\mathrm{grad}_x\,\mathrm{grad}_x^T[G_{k_s}(x,y)-G_{k_p}(x,y)]\\ &= \frac{1}{\mu}\begin{pmatrix}G_{k_s}(x,y) & 0\\ 0 & G_{k_s}(x,y)\end{pmatrix} + \frac{1}{\omega^2}\begin{pmatrix}\partial_{x_1}^2 & \partial_{x_1}\partial_{x_2}\\ \partial_{x_2}\partial_{x_1} & \partial_{x_2}^2\end{pmatrix}[G_{k_s}(x,y)-G_{k_p}(x,y)]. \end{aligned} \tag{3.2}$$

To split the function $x\to\Pi(x,y)$ into its compressional and shear parts, we rewrite $\Pi(x,y)$ as

$$\begin{aligned}\Pi(x,y) = &\sum_{n\in\mathbb{Z}}\left\{(\alpha_n,\beta_n)^T P^{(n)}(y)W_{p,n}\exp(\mathrm{i}(\alpha_n x_1+\beta_n x_2))\right\}\\ &+\sum_{n\in\mathbb{Z}}\left\{(-\gamma_n,\alpha_n)^T S^{(n)}(y)W_{s,n}\exp(\mathrm{i}(\alpha_n x_1+\gamma_n x_2))\right\}\end{aligned} \tag{3.3}$$

for $x_2>y_2$, where $P^n(y), S^n(y)\in\mathbb{C}^{2\times 1}$ will be referred to as the Rayleigh coefficients of the compressional and shear parts of $\Pi(x,y)$, respectively. Inserting the representation of $G_k(x,y)$ into (3.2), we find

$$\begin{aligned}P^n(y) &= \frac{\mathrm{i}}{4\pi\omega^2 W_{p,n}\beta_n}(\alpha_n,\beta_n)^T\exp(-\mathrm{i}\alpha_n y_1-\mathrm{i}\beta_n y_2),\\ S^n(y) &= \frac{\mathrm{i}}{4\pi\omega^2 W_{s,n}\gamma_n}(-\gamma_n,\alpha_n)^T\exp(-\mathrm{i}\alpha_n y_1-\mathrm{i}\gamma_n y_2)\end{aligned} \tag{3.4}$$

for $x_2 > y_2$. It is worth pointing out that the difference $\Pi(x, y) - \Pi(x, y')$ is not the half-space Green's tensor to the Navier equation since it does not vanish on Γ_0 by virtue of the derivative with respect to x_2 acting on G_{k_s} and G_{k_p}. In [4], making use of the Fourier transform, Arens has derived the non-quasi-periodic half-plane Green's tensor of the form

$$\Gamma_D(x, y) = \Gamma(x, y) - \Gamma(x, y') + U(x, y), \quad x \neq y, \quad x_2, y_2 > 0, \tag{3.5}$$

with the correction term $U(x, y)$ defined as the integral

$$U(x, y) := -\frac{\mathrm{i}}{2\pi\omega^2}\int_{-\infty}^{\infty}(M_p(t, \eta_p(t), \eta_s(t); x_2, y_2) + M_s(t, \eta_p(t), \eta_s(t); x_2, y_2))\mathrm{e}^{-\mathrm{i}(x_1-y_1)t}\mathrm{d}t,$$

$$M_p(t, \eta_p(t), \eta_s(t); x_2, y_2) := \frac{\mathrm{e}^{\mathrm{i}\eta_p(t)(x_2+y_2)} - \mathrm{e}^{\mathrm{i}(\eta_p(t)x_2+\eta_s(t)y_2)}}{\eta_p(t)\eta_s(t) + t^2}\begin{pmatrix} -t^2\eta_s(t) & t^3 \\ t\eta_p(t)\eta_s(t) & -t^2\eta_p(t) \end{pmatrix},$$

$$M_s(t, \eta_p(t), \eta_s(t); x_2, y_2) := \frac{\mathrm{e}^{\mathrm{i}\eta_s(t)(x_2+y_2)} - \mathrm{e}^{\mathrm{i}(\eta_s(t)x_2+\eta_p(t)y_2)}}{\eta_p(t)\eta_s(t) + t^2}\begin{pmatrix} -t^2\eta_s(t) & -t\eta_p(t)\eta_s(t) \\ -t^3 & -t^2\eta_p(t) \end{pmatrix},$$

where

$$\eta_p(t) := \begin{cases} \sqrt{k_p^2 - t^2}, & t^2 \leqslant k_p^2, \\ \mathrm{i}\sqrt{t^2 - k_p^2}, & t^2 > k_p^2, \end{cases} \qquad \eta_s(t) := \begin{cases} \sqrt{k_s^2 - t^2}, & t^2 \leqslant k_s^2, \\ \mathrm{i}\sqrt{t^2 - k_s^2}, & t^2 > k_s^2. \end{cases}$$

Motivated by the expression of Γ_D, we define the half-space α-quasi-periodic Green's tensor in the following way:

$$\Pi_D(x, y) := \sum_{n\in\mathbb{Z}}\exp(-\mathrm{i}\alpha 2\pi n)\Gamma_D(x + n(2\pi, 0), y) = \Pi(x, y) - \Pi(x, y') + U_\alpha(x, y)$$

for $x - y \neq n(2\pi, 0)^T$, $n \in \mathbb{Z}$, where

$$U_\alpha(x, y) := \sum_{n\in\mathbb{Z}}\exp(-\mathrm{i}\alpha 2\pi n)U(x + n(2\pi, 0), y). \tag{3.6}$$

From Poisson's summation formula, it is seen that

$$\sum_{n\in\mathbb{Z}}[\exp(-\mathrm{i}\alpha 2\pi n)\exp(-\mathrm{i}(x_1 + 2n\pi - y_1)t)] = \exp(-\mathrm{i}(x_1 - y_1)t)\sum_{n\in\mathbb{Z}}\delta(t + \alpha_n),$$

where $\delta(\cdot)$ denotes the Dirac delta function. Inserting the previous identity back into (3.6) yields an alternative expression of U_α:

$$\begin{aligned} U_\alpha(x, y) := \frac{\mathrm{i}}{2\pi\omega^2}\sum_{n\in\mathbb{Z}}\Bigg\{\Bigg[&\mathrm{e}^{\mathrm{i}(\alpha_n x_1+\beta_n x_2)}(\mathrm{e}^{-\mathrm{i}(\alpha_n y_1-\beta_n y_2)} - \mathrm{e}^{-\mathrm{i}(\alpha_n y_1-\gamma_n y_2)})\begin{pmatrix} \alpha_n\gamma_n & \alpha_n^2 \\ \beta_n\gamma_n & \alpha_n\beta_n \end{pmatrix} \\ &+\mathrm{e}^{\mathrm{i}(\alpha_n x_1+\gamma_n x_2)}(\mathrm{e}^{-\mathrm{i}(\alpha_n y_1-\gamma_n y_2)} - \mathrm{e}^{-\mathrm{i}(\alpha_n y_1-\beta_n y_2)})\begin{pmatrix} \alpha_n\gamma_n & -\gamma_n\beta_n \\ -\alpha_n^2 & \alpha_n\beta_n \end{pmatrix}\Bigg]\frac{\alpha_n}{\alpha_n^2 + \beta_n\gamma_n}\Bigg\} \end{aligned}$$

for $x_2 > y_2$. Hence, the nth Rayleigh coefficients of the compressional and shear parts of the function $x \to U_\alpha(x, y)$ can be formulated as (cf (2.8))

$$\tilde{P}^{(n)}(y) = \frac{\mathrm{i}\alpha_n}{2\pi\omega^2}\frac{\mathrm{e}^{-\mathrm{i}(\alpha_n y_1-\beta_n y_2)} - \mathrm{e}^{-\mathrm{i}(\alpha_n y_1-\gamma_n y_2)}}{W_{p,n}(\alpha_n^2 + \beta_n\gamma_n)}(\gamma_n, \alpha_n)^T,$$

$$\tilde{S}^{(n)}(y) = -\frac{\mathrm{i}\alpha_n}{2\pi\omega^2}\frac{\mathrm{e}^{-\mathrm{i}(\alpha_n y_1-\beta_n y_2)} - \mathrm{e}^{-\mathrm{i}(\alpha_n y_1-\gamma_n y_2)}}{W_{s,n}(\alpha_n^2 + \beta_n\gamma_n)}(-\alpha_n, \beta_n)^T$$

for $x_2 > y_2$ with $W_{p,n}, W_{s,n}$ given by (2.6).

To introduce our admissible sets of incident waves, as mentioned at the beginning of this section, we define $u_{1,n}^{\mathrm{in}}(y)$ and $u_{2,n}^{\mathrm{in}}(y)$ as the conjugate of the nth Rayleigh coefficient of the compressional and shear parts of the function $x \to \Pi_D(x, y)$, respectively. That is, after changing variables,

$$u^{\rm in}_{1,n}(x) := \overline{P^{(n)}(x) - P^{(n)}(x') + \tilde{P}^{(n)}(x)}, \quad u^{\rm in}_{2,n}(x) := \overline{S^{(n)}(x) - S^{(n)}(x') + \tilde{S}^{(n)}(x)} \tag{3.7}$$

for $n \in \mathbb{Z}$, where $P^{(n)}$ and $S^{(n)}$ are defined as in (3.4). More precisely, we can write $u^{\rm in}_{1,n}$ and $u^{\rm in}_{2,n}$ as

$$\begin{aligned} u^{\rm in}_{1,n}(x) &= \frac{-{\rm i}}{4\pi\omega^2\overline{\beta}_n\overline{W}_{p,n}}\big(u^{\rm in}_{1,n,{\rm d}}(x) + u^{\rm in}_{1,n,{\rm u}}(x)\big),\\ u^{\rm in}_{2,n}(x) &= \frac{-{\rm i}}{4\pi\omega^2\overline{\gamma}_n\overline{W}_{s,n}}\big(u^{\rm in}_{2,n,{\rm d}}(x) + u^{\rm in}_{2,n,{\rm u}}(x)\big), \end{aligned} \tag{3.8}$$

with $u^{\rm in}_{j,n,{\rm d}}$ and $u^{\rm in}_{j,n,{\rm u}}$, $j = 1, 2$, $n \in \mathbb{Z}$, denoting the downward and upward propagating modes, respectively, given by

$$u^{\rm in}_{1,n,{\rm d}}(x) = \begin{cases} \frac{\alpha_n^2-\beta_n\gamma_n}{\alpha_n^2+\beta_n\gamma_n}\begin{pmatrix}-\alpha_n\\ \beta_n\end{pmatrix}{\rm e}^{{\rm i}(\alpha_n x_1-\beta_n x_2)} - \frac{2\alpha_n\beta_n}{\alpha_n^2+\beta_n\gamma_n}\begin{pmatrix}\gamma_n\\ \alpha_n\end{pmatrix}{\rm e}^{{\rm i}(\alpha_n x_1-\gamma_n x_2)}, & |\alpha_n| \leqslant k_p,\\ \begin{pmatrix}\alpha_n\\ -\beta_n\end{pmatrix}{\rm e}^{{\rm i}(\alpha_n x_1-\beta_n x_2)} + \frac{2\alpha_n\beta_n}{\alpha_n^2-\beta_n\gamma_n}\begin{pmatrix}\gamma_n\\ \alpha_n\end{pmatrix}{\rm e}^{{\rm i}(\alpha_n x_1-\gamma_n x_2)}, & k_p < |\alpha_n| < k_s,\\ \begin{pmatrix}\alpha_n\\ -\beta_n\end{pmatrix}{\rm e}^{{\rm i}(\alpha_n x_1-\beta_n x_2)}, & |\alpha_n| \geqslant k_s, \end{cases}$$

$$u^{\rm in}_{1,n,{\rm u}}(x) = \begin{cases} \begin{pmatrix}\alpha_n\\ \beta_n\end{pmatrix}{\rm e}^{{\rm i}(\alpha_n x_1+\beta_n x_2)}, & |\alpha_n| \leqslant k_p,\\ -\frac{\alpha_n^2+\beta_n\gamma_n}{\alpha_n^2-\beta_n\gamma_n}\begin{pmatrix}\alpha_n\\ \beta_n\end{pmatrix}{\rm e}^{{\rm i}(\alpha_n x_1+\beta_n x_2)}, & k_p < |\alpha_n| < k_s,\\ -\frac{\alpha_n^2-\beta_n\gamma_n}{\alpha_n^2+\beta_n\gamma_n}\begin{pmatrix}\alpha_n\\ \beta_n\end{pmatrix}{\rm e}^{{\rm i}(\alpha_n x_1+\beta_n x_2)} - \frac{2\alpha_n\beta_n}{\alpha_n^2+\beta_n\gamma_n}\begin{pmatrix}\gamma_n\\ -\alpha_n\end{pmatrix}{\rm e}^{{\rm i}(\alpha_n x_1+\gamma_n x_2)}, & |\alpha_n| \geqslant k_s, \end{cases}$$

and

$$u^{\rm in}_{2,n,{\rm d}}(x) = \begin{cases} \frac{\alpha_n^2-\beta_n\gamma_n}{\alpha_n^2+\beta_n\gamma_n}\begin{pmatrix}\gamma_n\\ \alpha_n\end{pmatrix}{\rm e}^{{\rm i}(\alpha_n x_1-\gamma_n x_2)} - \frac{2\alpha_n\gamma_n}{\alpha_n^2+\beta_n\gamma_n}\begin{pmatrix}\alpha_n\\ -\beta_n\end{pmatrix}{\rm e}^{{\rm i}(\alpha_n x_1-\beta_n x_2)}, & |\alpha_n| \leqslant k_p,\\ \frac{\alpha_n^2+\beta_n\gamma_n}{\alpha_n^2-\beta_n\gamma_n}\begin{pmatrix}\gamma_n\\ \alpha_n\end{pmatrix}{\rm e}^{{\rm i}(\alpha_n x_1-\gamma_n x_2)}, & k_p < |\alpha_n| < k_s,\\ -\begin{pmatrix}\gamma_n\\ \alpha_n\end{pmatrix}{\rm e}^{{\rm i}(\alpha_n x_1-\gamma_n x_2)}, & |\alpha_n| \geqslant k_s, \end{cases}$$

$$u^{\rm in}_{2,n,{\rm u}}(x) = \begin{cases} \begin{pmatrix}\gamma_n\\ -\alpha_n\end{pmatrix}{\rm e}^{{\rm i}(\alpha_n x_1+\gamma_n x_2)}, & |\alpha_n| \leqslant k_p,\\ \begin{pmatrix}\gamma_n\\ -\alpha_n\end{pmatrix}{\rm e}^{{\rm i}(\alpha_n x_1+\gamma_n x_2)} - \frac{2\alpha_n\gamma_n}{\alpha_n^2-\beta_n\gamma_n}\begin{pmatrix}\alpha_n\\ \beta_n\end{pmatrix}{\rm e}^{{\rm i}(\alpha_n x_1+\beta_n x_2)}, & k_p < |\alpha_n| < k_s,\\ \frac{\alpha_n^2-\beta_n\gamma_n}{\alpha_n^2+\beta_n\gamma_n}\begin{pmatrix}-\gamma_n\\ \alpha_n\end{pmatrix}{\rm e}^{{\rm i}(\alpha_n x_1+\gamma_n x_2)} + \frac{2\alpha_n\gamma_n}{\alpha_n^2+\beta_n\gamma_n}\begin{pmatrix}\alpha_n\\ \beta_n\end{pmatrix}{\rm e}^{{\rm i}(\alpha_n x_1+\beta_n x_2)}, & |\alpha_n| \geqslant k_s. \end{cases}$$

It can be readily checked that the $u^{\rm in}_{j,n}$ are α-quasi-periodic solutions to the Navier equation with the Dirichlet boundary condition on Γ_0. Note that, for the inverse problems $(\mathbf{P}_j)$ and $(\mathbf{S}_j)$, $j = 1, 2$, both compressional and shear waves are involved in the incident elastic waves $u^{\rm in}_{j,n}$, $n \in \mathbb{Z}$, although the measurement data only come from the compressional part when $j = 1$ or the shear part in the case $j = 2$.

Since the upward propagating modes occurring in the $u^{\rm in}_{j,n}$ $(j = 1, 2)$ are not physically meaningful incoming waves from Ω_Λ, the scattered field $u^{\rm sc}_{j,n}$ due to $u^{\rm in}_{j,n}$ cannot be generated straightforwardly. Denoting by $\widetilde{u}^{\rm sc}_{j,n}$ the scattered field corresponding to $u^{\rm in}_{j,n,\rm d}$, we have

$$u^{\rm sc}_{1,n} = \frac{-\mathrm{i}}{4\pi\omega^2\overline{\beta}_n\overline{W}_{p,n}}\left(\widetilde{u}^{\rm sc}_{1,n} - u^{\rm in}_{1,n,\rm u}\right), \quad u^{\rm sc}_{2,n} = \frac{-\mathrm{i}}{4\pi\omega^2\overline{\gamma}_n\overline{W}_{s,n}}\left(\widetilde{u}^{\rm sc}_{2,n} - u^{\rm in}_{2,n,\rm u}\right), \quad n \in \mathbb{Z},$$

due to the linearity of the scattering solution with respect to the incident waves. Consequently, the mth Rayleigh coefficients $A^{j,n}_{p,m}$ and $A^{j,n}_{s,m}$ of $u^{\rm sc}_{j,n}$ can be written as

$$A^{j,n}_{p,m} = \frac{-\mathrm{i}}{4\pi\omega^2\overline{\beta}_n W_{p,n}}\left(\widetilde{A}^{j,n}_{p,m} - \widehat{A}^{p,n}_{p,m}\right), \quad A^{j,n}_{s,m} = \frac{-\mathrm{i}}{4\pi\omega^2\overline{\gamma}_n W_{s,n}}\left(\widetilde{A}^{j,n}_{s,m} - \widehat{A}^{p,n}_{s,m}\right)$$

for $m, n \in \mathbb{Z}$, $j = 1, 2$, where $\widetilde{A}^{j,n}_{p,m}$ and $\widehat{A}^{j,n}_{p,m}$ (resp. $\widetilde{A}^{j,n}_{s,m}$ and $\widehat{A}^{j,n}_{s,m}$) denote the mth Rayleigh coefficients of the compressional (resp. shear) part of $\tilde{u}^{\rm sc}_{j,n}$ and $u^{\rm in}_{j,n,\rm u}$, respectively.

4. The factorization method

Since the inverse problems $(\mathbf{P}_j)$ and $(\mathbf{S}_j)$ $(j = 1, 2, 3)$ are very similar, we only consider the inverse problems $(\mathbf{P}_j)$. With necessary modifications on the quasi-periodicity, the mathematical argument automatically carries over to the inverse problems $(\mathbf{S}_j)$. Thus, unless otherwise stated we always assume $\alpha = k_p \sin\theta$ for some fixed $\theta \in (-\pi/2, \pi/2)$. The unknown grating profile Λ will be recovered from the information of the Rayleigh coefficients of the scattered P- or S-waves, corresponding to each incident elastic wave from the admissible set $\mathcal{I}_1(\alpha)$ or $\mathcal{I}_2(\alpha)$ of α-quasi-periodic functions introduced in section 3.

Thanks to the periodicity of the grating profile and the α-quasi-periodicity of the solutions, our discussion is restricted to one periodic cell. Consequently, we redefine the region and the boundary as

$$\begin{aligned}
&\Omega_\Lambda := \{x \in \mathbb{R}^2\ :\ x_1 \in (0, 2\pi), x_2 > f(x_1) > 0\},\\
&\Lambda := \{x \in \mathbb{R}^2\ :\ x_1 \in (0, 2\pi), x_2 = f(x_1)\},\\
&\Gamma_h := \{x \in \mathbb{R}^2\ :\ x_1 \in (0, 2\pi), x_2 = h\}
\end{aligned}$$

for some $h > \Lambda^+ > 0$. Analogously, we set $\mathbb{R}^2_\pi := \{y = (y_1, y_2) \in \mathbb{R}^2\ :\ 0 < y_1 < 2\pi\}$. Introduce the domain $\Omega_h := \Omega^+_h \cup \Lambda \cup \Omega^-_{-h}$, where

$$\begin{aligned}
&\Omega^+_h := \{x \in \mathbb{R}^2 : x_1 \in (0, 2\pi),\ 0 < f(x_1) < x_2 < h\},\\
&\Omega^-_{-h} := \{x \in \mathbb{R}^2 : x_1 \in (0, 2\pi),\ -h < x_2 < f(x_1)\}.
\end{aligned}$$

With Green's tensor Π, we define the periodic single-layer potential

$$(\mathrm{SL}\varphi)(x) := \int_\Lambda \Pi(x, y)\varphi(y)\,\mathrm{d}s(y), \quad x \in \mathbb{R}^2_\pi, \tag{4.1}$$

and the corresponding single-layer boundary operator

$$\mathcal{S}\varphi(x) = \int_\Lambda \Pi(x, y)\varphi(y)\,\mathrm{d}s(y), \quad x \in \Lambda.$$

Similarly, one can define the integral operators SL_D and $\mathcal{S}_D$ with the kernel Π replaced by the half-space Green's tensor Π_D, i.e.,

$$\begin{aligned}
&(\mathrm{SL}_D\varphi)(x) := \int_\Lambda \Pi_D(x, y)\varphi(y)\,\mathrm{d}s(y), \quad x \in \mathbb{R}^2_\pi,\\
&\mathcal{S}_D\varphi(x) := \int_\Lambda \Pi_D(x, y)\varphi(y)\,\mathrm{d}s(y), \quad x \in \Lambda.
\end{aligned}$$

In what follows, we sometimes employ the notation $\mathrm{SL}^{(\omega)}$, $\mathrm{SL}_D^{(\omega)}$, $\mathcal{S}^{(\omega)}$ and $\mathcal{S}_D^{(\omega)}$ to indicate their dependence on the frequency ω.

For $s \in \mathbb{R}$, let $H_\alpha^s(\cdot)$ denote the Sobolev spaces of scalar functions in the domain $(\cdot)$ which are α-quasi-periodic with respect to x_1. Analogously to the factorization method for bounded obstacle scattering problems, we now define the periodic version of the so-called data-to-pattern operator G_j, the Herglotz operator H_j and the near-field operator N_j for $(\mathbf{P}_j)$, $j = 1, 2, 3$.

Definition 4.1. *The data-to-pattern operators* $G_j : H_\alpha^{1/2}(\Lambda)^2 \to l^2$, $j = 1, 2$, *are defined as*

$$G_1(\varphi) = \{A_{p,n} : n \in \mathbb{Z}\}, \quad G_2(\varphi) = \{A_{s,n} : n \in \mathbb{Z}\} \quad \textit{for} \quad \varphi \in H_\alpha^{1/2}(\Lambda)^2,$$

where $A_{p,n}$ *(resp.* $A_{s,n}$*) denote the nth Rayleigh coefficients of the compressional (resp. shear) part of the unique scattered field* u^{sc} *to problem (2.2)–(2.5) with the boundary value data* $u^{\mathrm{sc}} = \varphi$ *on* Λ*. The operator* $G_3 : H_\alpha^{1/2}(\Lambda)^2 \to l^2 \times l^2$ *is defined as the product of* G_1 *and* G_2*, that is,* $G_3 := G_1 \times G_2$.

Definition 4.2. *With the incident waves* $u_{j,n}^{\mathrm{in}}$ *given in (3.8), the Herglotz operators* $H_j : l^2 \to H_\alpha^{1/2}(\Lambda)^2$ *for* $j = 1, 2$ *and* $H_3 : l^2 \times l^2 \to H_\alpha^{1/2}(\Lambda)^2$ *are defined as*

$$[H_j(\boldsymbol{b})](x) := \sum_{n\in\mathbb{Z}} b_n u_{j,n}^{\mathrm{in}}(x), \quad j = 1, 2, \quad H_3(\boldsymbol{a}, \boldsymbol{b}) := H_1(\boldsymbol{a}) + H_2(\boldsymbol{b}), \quad x \in \Lambda$$

for $\boldsymbol{a} = (a_n)_{n\in\mathbb{Z}}$, $\boldsymbol{b} = (b_n)_{n\in\mathbb{Z}} \in l^2$.

Definition 4.3. *Define the near-field operators* $N_j : l^2 \to l^2$, $j = 1, 2$, *and* $N_3 : l^2 \times l^2 \to l^2 \times l^2$ *as*

$$N_j = -G_j H_j, \quad j = 1, 2, 3.$$

The Herglotz operator H_3 is a combination of $k_p \sin\theta$-quasi-periodic incident waves $u_{1,n}^{\mathrm{in}}$ and the $k_s \sin\theta$-quasi-periodic ones $u_{2,n}^{\mathrm{in}}$ with different weights. The near-field operator N_j ($j = 1, 2$) maps the combination of the incident waves $u_{j,n}^{\mathrm{in}}$ to the Rayleigh coefficients of the compressional part ($j = 1$) or the shear part ($j = 2$) of the associated scattered field.

Take a fixed vector $\mathbf{C} \in \mathbb{C}^{2\times 1}$ and some point $y = (y_1, y_2) \in \mathbb{R}_\pi^2$. In view of Green's tensor $\Pi(x, y)$ given in (3.3), we can explicitly formulate the Rayleigh coefficients $C_{p,n}(y)$ and $C_{s,n}(y)$ of the compressional and shear parts of the function $x \to \Pi(x, y)\mathbf{C}$ as

$$\begin{aligned} C_{p,n}(y) &= \frac{\mathrm{i}}{4\pi\omega^2\beta_n W_{p,n}} \exp(-\mathrm{i}y \cdot (\alpha_n, \beta_n)^T)[(\alpha_n, \beta_n)^T \cdot \mathbf{C}], \\ C_{s,n}(y) &= \frac{\mathrm{i}}{4\pi\omega^2\gamma_n W_{s,n}} \exp(-\mathrm{i}y \cdot (\alpha_n, \gamma_n)^T)[(-\gamma_n, \alpha_n)^T \cdot \mathbf{C}] \end{aligned} \tag{4.2}$$

for $x_2 > y_2 > 0$. The sequences $C_{p,n}$ and $C_{s,n}$ will be utilized to characterize the region beneath the periodic scattering surface.

Lemma 4.4. *Assume* $\boldsymbol{C} \in \mathbb{C}^{2\times 1}$ *is a non-zero complex vector and* $y \in \mathbb{R}_\pi^2$*. Then,*

$$\begin{aligned} \{C_{p,n}(y)\}_{n\in\mathbb{Z}} &\in \mathcal{R}[G_1] \Leftrightarrow y \in \mathbb{R}_\pi^2 \backslash \overline{\Omega}_\Lambda, \\ \{C_{s,n}(y)\}_{n\in\mathbb{Z}} &\in \mathcal{R}[G_2] \Leftrightarrow y \in \mathbb{R}_\pi^2 \backslash \overline{\Omega}_\Lambda, \\ \{C_{p,n}(y)\}_{n\in\mathbb{Z}} \times \{C_{s,n}(y)\}_{n\in\mathbb{Z}} &\in \mathcal{R}[G_3] \Leftrightarrow y \in \mathbb{R}_\pi^2 \backslash \overline{\Omega}_\Lambda. \end{aligned}$$

Here, the notation $\mathcal{R}[\cdot]$ *denotes the range of an operator.*

Proof. We only need to consider the sequence $\{C_{p,n}(y)\ :\ n \in \mathbb{Z}\}$ since the other cases can be dealt with in the same manner. Obviously, we have $\{C_{p,n}(y)\ :\ n \in \mathbb{Z}\} \in l^2$ whenever $y_2 < h$. If $y \in \mathbb{R}^2_\pi \backslash \overline{\Omega}_\Lambda$, then $\{C_{p,n}(y)\ :\ n \in \mathbb{Z}\} = N_1(\varphi)$ with $\varphi = (\Pi(x, y)\mathbf{C})|_\Lambda \in H^{1/2}_\alpha(\Lambda)^2$.

Assume that $\{C_{p,n}(y) : n \in \mathbb{Z}\} = N_1(\tilde{\varphi})$ for some $\tilde{\varphi} \in H^{1/2}_\alpha(\Lambda)^2$ and $y \in \overline{\Omega^+_h}$. Denote by $\Pi^C_P(x)$ the pressure part of the function $\Pi(x, y)\mathbf{C}$ restricted to Γ_h and by u^{sc} the scattered field of problem (2.2)–(2.5) with the boundary data $u^{\mathrm{sc}} = \tilde{\varphi}$ on Λ. The coincidence of Π^C_P with the compressional part u^{sc}_p of u^{sc} on Γ_h implies that $\Pi^C_P(x) = u^{\mathrm{sc}}_p$ in $x_2 > h$, due to the uniqueness of the Dirichlet boundary value problem in a half-plane. Together with the unique continuation of solutions to the Helmholtz equation, this further yields the fact that $\Pi^C_P(x) = u^{\mathrm{sc}}_p$ in $\Omega^+_h \backslash \{y\}$. On one hand, we have $\operatorname{div} u^{\mathrm{sc}}_p = \operatorname{div} u^{\mathrm{sc}} \in L^2_{\mathrm{loc}}(\Omega^+_h)$. On the other hand, there holds $\operatorname{div} \Pi^C_P(x) = \operatorname{div}_x[\Pi(x, y)\mathbf{C}] \notin L^2_{\mathrm{loc}}(\Omega^+_h)$ since the shear part of u^{sc} is divergence-free and $\operatorname{div}_x[\Pi(x, y)\mathbf{C}] \sim \mathcal{O}(|x - y|^{-1})$ as $x \to y$ in $\Omega^+_h \backslash \{y\}$. This contradiction implies that $y \in \mathbb{R}^2_\pi \backslash \overline{\Omega}_\Lambda$. □

By lemma 4.4, the grating profile Λ can be identified theoretically from the ranges of G_j for any $j = 1, 2, 3$, which, however, cannot be numerically implemented. Note that only the near-field operators N_j can be discretized from knowledge of the Rayleigh coefficients due to the admissible incident waves. The essence of the factorization method is to connect the range of N_j with that of G_j so that the grating profile can be retrieved from the spectrum of N_j. To this end, we will factorize N_j in terms of G_j as shown in the following lemma. In the following, H^*_j $(j = 1, 2, 3)$ denotes the adjoint operator of H_j. Recall that $\mathcal{S}_D$ stands for the single-layer boundary operator whose kernel is the half-space Green's tensor Π_D.

Lemma 4.5. *It holds that $H^*_j = G_j\mathcal{S}_D$ and the factorization $N_j = -G_j\mathcal{S}^*_D G^*_j$ for $j = 1, 2, 3$.*

Proof. For $\varphi \in H^{-1/2}_\alpha(\Lambda)^2$, let $(G_j\mathcal{S}_D\varphi)_n$ represent the nth Rayleigh coefficient of $G_j\mathcal{S}_D(\varphi)$, $j = 1, 2$. From the definition of $\mathcal{S}_D$, G_j and $u^{\mathrm{in}}_{j,n}$, we deduce that (cf (3.7))

$$(G_j\mathcal{S}_D\varphi)_n = \int_\Lambda \overline{u^{\mathrm{in}}_{j,n}} \cdot \varphi \,\mathrm{d}s, \qquad j = 1, 2.$$

The relations $H^*_j = G_j\mathcal{S}_D$, $j = 1, 2$, then follow directly from the previous identity and the definition of H_j. This further yields the factorization $N_j = -G_jH_j = -G_j\mathcal{S}^*_D G^*_j$. From the definitions of H_3 and G_3, we arrive at the result that $H^*_3 = H^*_1 \times H^*_2 = G_3\mathcal{S}_D$. Thus, $N_3 = -G_3H_3 = -G_3\mathcal{S}^*_D G^*_3$. □

We now introduce the concept of the Dirichlet eigenvalue for quasi-periodic Lamé operators over a periodic domain.

Definition 4.6. *The frequency ω of an incidence wave is called a Dirichlet eigenvalue of the α-quasi-periodic Lamé operator over the periodic layer $\Omega^-_0 := \{x : 0 < x_2 < f(x_1), 0 < x_1 < 2\pi\}$ if there exists a non-trivial α-quasi-periodic solution u to the Navier equation (2.2) on Ω^-_0 such that $u = 0$ on Λ and Γ_0. Accordingly, u is called the Dirichlet eigenfunction with the phase-shift α.*

Using variational arguments and standard spectral theory for compact operators, one can show that the Dirichlet eigenvalues form a countable set and the positive eigenvalues can be represented in terms of a min–max principle (see [2]). A further investigation of the monotonicity of these eigenvalues in [2] leads to Schiffer's uniqueness theorem for the inverse elastic scattering by rigid periodic surfaces. For the inverse problems ($\mathbf{P}_j$), we make the following assumption.

Assumption (A). The frequency ω is not a Dirichlet eigenvalue of the quasi-periodic Lamé operator over the periodic region Ω_0^- with the phase-shift $\alpha = k_p \sin\theta$.

This assumption will be used to verify the injectivity of the single-layer boundary operator $\mathcal{S}_D$, see lemma (4.7) (iii) and remark 4.8 below. Before describing the properties of the middle operator $\mathcal{S}_D^*$ involved in the factorization $N_j = -G_j\mathcal{S}_D^*G_j^*$, we recall that the real and imaginary parts of an operator T on a Hilbert space are given by

$$\mathrm{Re}(T) := (T + T^*)/2, \quad \mathrm{Im}(T) := (T - T^*)/(2\mathrm{i}).$$

Let the dual form $\langle\cdot,\cdot\rangle$ denote the dual pair between $H_\alpha^{-1/2}(\Lambda)^2$ and $H_\alpha^{1/2}(\Lambda)^2$ which extends the inner product of $L^2(\Lambda)^2$.

Lemma 4.7. *(i) There exist an angle $\phi \in (0, \pi/2)$ and a sufficiently small frequency $\omega_0 > 0$ such that the real part of the operator $\exp(-\mathrm{i}\phi)\mathcal{S}^{(\omega)}$ is self-adjoint and positive definite when $\omega \in (0, \omega_0]$. Particularly, there exists a constant $c > 0$ such that*

$$\mathrm{Re}\langle\varphi, \exp(-i\phi)\mathcal{S}^{(\omega)}\varphi\rangle \geqslant c\omega\|\varphi\|^2_{H_\alpha^{-1/2}(\Lambda)^2}, \quad \forall\varphi \in H_\alpha^{-1/2}(\Lambda)^2, \forall\omega \in (0, \omega_0]. \tag{4.3}$$

(ii) For any $\omega_1 \in (0, \omega_0]$, the operator $\mathcal{S_D}^{(\omega)} - \mathcal{S}^{(\omega_1)}$ is compact from $H_\alpha^{-1/2}(\Lambda)^2$ to $H_\alpha^{1/2}(\Lambda)^2$ and thus $\mathcal{S}_D^{(\omega)}$ is a Fredholm operator with index zero for any $\omega \in \mathbb{R}^+$.

(iii) Under the assumption (A), the middle operator $-\mathcal{S}_D^* : H_\alpha^{-1/2}(\Lambda)^2 \to H_\alpha^{1/2}(\Lambda)^2$ is injective.

(iv) $-\mathrm{Im}(\mathcal{S}_D^*)$ is non-negative over $H_\alpha^{-1/2}(\Lambda)^2$, that is,

$$-\langle\varphi, \mathrm{Im}(\mathcal{S}_D^*)\varphi\rangle \geqslant 0 \quad \textit{for all} \quad \varphi \in H_\alpha^{-1/2}(\Lambda)^2.$$

Proof. (i) Define $u(x) := \mathrm{SL}^{(\omega)}\varphi(x),\ x \in \mathbb{R}^2_\pi$. Then, u satisfies the Navier equation in $\mathbb{R}^2_\pi\backslash\Lambda$, the upward Rayleigh expansion (2.5) for $x_2 > \Lambda^+$ and an analogous downward Rayleigh expansion in $x_2 < \Lambda^- := \min_{x\in\Lambda}\{x_2\}$. From the first Betti's formula and the jump relations for periodic single-layer potentials, it follows that

$$\begin{aligned}\langle\varphi, \mathcal{S}^{(\omega)}\varphi\rangle &= \int_\Lambda (\partial_\nu u^+ - \partial_\nu u^-)\cdot\overline{u}\,\mathrm{d}s\\ &= \int_{\Omega_h} [\mathcal{E}(u,\overline{u}) - \omega^2|u|^2]\,\mathrm{d}x - \int_{\Gamma_h} \mathcal{T}_\omega^+ u\cdot\overline{u}\,\mathrm{d}s - \int_{\Gamma_{-h}} \mathcal{T}_\omega^- u\cdot\overline{u}\,\mathrm{d}s,\end{aligned} \tag{4.4}$$

where $\Omega_h = \{x \in \mathbb{R}^2_\pi\ :\ -h < x_2 < h\}$. In (4.4), the bilinear form $\mathcal{E}(\cdot,\cdot)$ is defined as

$$\begin{aligned}\mathcal{E}(u, v) = {}&(2\mu+\lambda)(\partial_1 u_1\partial_1 v_1 + \partial_2 u_2\partial_2 v_2) + \mu(\partial_2 u_1\partial_2 v_1 + \partial_1 u_2\partial_1 v_2)\\ &+\mu(\partial_2 u_1\partial_1 v_2 + \partial_1 u_2\partial_2 v_1) + \lambda(\partial_1 u_1\partial_2 v_2 + \partial_2 u_2\partial_1 v_1),\end{aligned}$$

and $\mathcal{T}_\omega^\pm$ are the Dirichlet-to-Neumann maps defined on $\Gamma_{\pm h}$, respectively, given by (see [11])

$$\mathcal{T}_\omega^\pm v = -\sum_{n\in\mathbb{Z}} M_{n,\omega}\widehat{v}_n\exp(\mathrm{i}\alpha_n x_1) \quad \text{for} \quad v = \sum_{n\in\mathbb{Z}}\widehat{v}_n\exp(\mathrm{i}\alpha_n x_1) \in H_\alpha^{1/2}(\Gamma_{\pm h})^2. \tag{4.5}$$

The matrices $M_{n,\omega} \in \mathbb{C}^{2\times 2}$ in (4.5) are of the form

$$M_{n,\omega} := \frac{1}{\mathrm{i}}\begin{pmatrix} \omega^2\beta_n/t_n & 2\mu\alpha_n - \omega^2\alpha_n/t_n\\ -2\mu\alpha_n + \omega^2\alpha_n/t_n & \omega^2\gamma_n/t_n\end{pmatrix}, \quad t_n = \alpha_n^2 + \beta_n\gamma_n. \tag{4.6}$$

Consequently,

$$\begin{aligned}\mathrm{Re}\langle\varphi, \exp(-\mathrm{i}\phi)\mathcal{S}^{(\omega)}\varphi\rangle = {}&\cos\phi\int_{\Omega_h}\left[\mathcal{E}(u,\overline{u}) - \omega^2|u|^2\right]\mathrm{d}x\\ &- \mathrm{Re}\left\{\exp(\mathrm{i}\phi)\int_{\Gamma_h\cup\Gamma_{-h}} \mathcal{T}_\omega^\pm u\cdot\overline{u}\,\mathrm{d}s\right\}.\end{aligned} \tag{4.7}$$

We claim that there exist $\phi \in (0, \pi/2)$ and $\omega_* > 0$ such that for all $u \in H^{1/2}_\alpha(\Gamma_{\pm h})^2$, $\omega \in (0, \omega_*]$ there holds the inequality

$$-\operatorname{Re}\left\{\exp(\mathrm{i}\phi)\int_{\Gamma_{\pm h}} \mathcal{T}^{\pm}_\omega u \cdot \overline{u}\, \mathrm{d}s\right\} \geqslant c\omega\|u\|^2_{H^{1/2}_\alpha(\Gamma_{\pm h})^2} \tag{4.8}$$

with some constant $c > 0$ independent of ω and u; see lemma A.1 (i) in the appendix for the proof. By the Friedrich-type inequality for the Navier equation (see, e.g., [11, remark 2]) and the trace lemma, it follows from (4.7) and (4.8) that

$$\begin{aligned}\operatorname{Re}\langle\varphi, \exp(-\mathrm{i}\phi)\mathcal{S}^{(\omega)}\varphi\rangle &\geqslant \widetilde{c}\omega\|u\|^2_{H^1(\Omega_h)^2} - \omega^2\|u\|^2_{L^2(\Omega_h)^2}\\ &\geqslant c\omega\|u\|^2_{H^1(\Omega_h)^2}\\ &\geqslant c\omega\|u\|^2_{H^{1/2}(\Lambda)^2},\end{aligned} \tag{4.9}$$

for some constants $\tilde{c}, c > 0$ and for all $\omega \in (0, \omega_0]$, with ω_0 being sufficiently small. Arguing in the same way as in [6], one can show that the single-layer boundary operator $S^{(\omega)} : H^{-1/2}_\alpha(\Lambda)^2 \to H^{1/2}_\alpha(\Lambda)^2$ is an isomorphism provided Λ is the graph of some function. Now the estimate (4.3) follows from (4.9) for some sufficiently small positive number ω_0.

(ii) We write $\mathcal{S}^{(\omega)}_D - \mathcal{S}^{(\omega_1)} = \mathcal{S}^{(\omega)}_D - \mathcal{S}^{(\omega)} + \mathcal{S}^{(\omega)} - \mathcal{S}^{(\omega_1)}$. From the definitions of $\mathcal{S}^{(\omega)}_D$ and $\mathcal{S}^{(\omega)}$, we see that the kernels of $\mathcal{S}^{(\omega)}_D - \mathcal{S}^{(\omega)}$ and $\mathcal{S}^{(\omega)} - \mathcal{S}^{(\omega_1)}$ are both smooth. Hence, $\mathcal{S}^{(\omega)}_D - \mathcal{S}^{(\omega_1)}$ is compact from $H^{-1/2}_\alpha(\Lambda)^2$ to $H^{1/2}_\alpha(\Lambda)^2$. By (i), $\mathcal{S}^{(\omega)}_D$ is a Fredholm operator with index zero.

(iii) Since $\mathcal{S}_D$ is a Fredholm operator with index zero, we have $\dim(\operatorname{Ker}(\mathcal{S}_D)) = \dim(\operatorname{Ker}(\mathcal{S}^*_D))$. Hence, it suffices to prove the injectivity of $\mathcal{S}_D$. Define the single-layer potential $u(x) = \mathrm{SL}_D\varphi(x)$ for $x \in \mathbb{R}^2_\pi$. If $\mathcal{S}_D\varphi = 0$ on Λ, then $u = 0$ on Λ. Moreover, we have $u = 0$ in Ω^+_h due to the uniqueness of the direct scattering problem. Observing that u satisfies the Navier equation on Ω^-_0 and vanishes on Λ and Λ_0, we obtain $u = 0$ in Ω^-_0 by assumption (A). The jump relations for SL_φ finally yield $\varphi = 0$ on Λ.

(iv) For $\varphi \in H^{-1/2}_\alpha(\Lambda)^2$, there holds

$$-\langle\varphi, \operatorname{Im}(\mathcal{S}^*_D)\varphi\rangle = \operatorname{Im}\langle\varphi, \mathcal{S}^*_D\varphi\rangle = \operatorname{Im}\langle\mathcal{S}_D\varphi, \varphi\rangle = -\operatorname{Im}\langle\varphi, \mathcal{S}_D\varphi\rangle.$$

Thus, we only need to prove that $-\operatorname{Im}\langle\varphi, \mathcal{S}_D\varphi\rangle \geqslant 0$. To this end, define $u(x) := \mathrm{SL}^{(\omega)}_D\varphi(x)$, $x \in \mathbb{R}^2_\pi$. Arguing similarly as in (i) with Γ_{-h} replaced by Γ_0 and using the fact that u vanishes on Γ_0, we obtain (see [11])

$$-\operatorname{Im}\langle\varphi, \mathcal{S}_D\varphi\rangle = \operatorname{Im}\int_{\Gamma_h} \mathcal{T}u \cdot \overline{u}\, \mathrm{d}s = 2\pi\omega^2\left(\sum_{|\alpha_n|<k_p} \beta_n|A_{p,n}|^2 + \sum_{|\alpha_n|<k_s} \gamma_n|A_{s,n}|^2\right) \geqslant 0,$$

where $A_{p,n}$ and $A_{s,n}$ denote the Rayleigh coefficients of the compressional and shear parts of u, respectively. □

Remark 4.8. To prove the injectivity of $\mathcal{S}_D$, we think it is necessary to make the assumption (**A**); see the proof of lemma 4.7 (iii). Note that the single-layer potential (4.1) consists of both upward and downward propagating modes in the region $-f(x_1) < x_2 < f(x_1)$ and is non-analytic on the two curves $x_2 = f(x_1)$ and $x_2 = -f(x_1)$. An analogous assumption to assumption (**A**) above could be used to close a gap in the proof of [5, lemma 2.5 (i)], where a half-space quasi-periodic Green's function for the Helmholtz equation is involved.

Before stating the range identity, we need the following compactness and denseness results of the data-to-pattern operators G_j.

Lemma 4.9. *The operators G_j for $j = 1, 2, 3$ are all compact and have a dense range.*

Lemma 4.9 can be proved in a standard way; see [28, chapter 2] for a proof in the inverse acoustic scattering from penetrable diffraction gratings, which can be readily adapted to the Navier equation case. Lemmas 4.7 and 4.9 allow us to directly apply the range identity of [30, theorem 3.4.1] to the factorization of the near-field operators N_j established in lemma 4.5. The following abstract range identity generalizes the one contained in [28, chapter 1], the proof of which is essentially based on the approach of Kirsch and Grinberg [25, theorem 2.15] (cf [30]).

Lemma 4.10 (Range identity). *Let $X \subset U \subset X^*$ be a Gelfand triple with the Hilbert space U and reflexive Banach space X such that the embedding is dense. Furthermore, let Y be a second Hilbert space and $F : Y \to Y$, $G : X \to Y$ and $T : X^* \to X$ be linear and bounded operators with $F = GTG^*$. Suppose further that*

(a) G is compact and has a dense range.
(b) There exists $t \in (0, 2\pi)$ with $\cos t \neq 0$ such that $\mathrm{Re}[\exp(\mathrm{i}t)T]$ has the form $\mathrm{Re}[\exp(\mathrm{i}t)T] = T_0 + T_1$ with some compact operator T_1 and some coercive operator $T_0 : X^* \to X$, that is, there exists $c > 0$ with

$$\langle \varphi, T_0\varphi\rangle \geqslant c\|\varphi\|^2 \quad \textit{for all} \quad X^*. \tag{4.10}$$

(c) $\mathrm{Im}(T)$ is non-negative on X, that is, $\langle \mathrm{Im}(T)\varphi, \varphi\rangle \geqslant 0$ for all $\varphi \in X$. Moreover, we assume that one of the following conditions is fulfilled.
(d) T is injective.
(e) $\mathrm{Im}(T)$ is positive on the finite-dimensional null space of $\mathrm{Re}[\exp(\mathrm{i}t)T]$, that is, for all $\varphi \neq 0$ such that $\mathrm{Re}[\exp(\mathrm{i}t)T]\varphi = 0$ we have $\langle \mathrm{Im}(T)\varphi, \varphi\rangle > 0$.

Then, the operator $F_\sharp := |\mathrm{Re}[\exp(\mathrm{i}t)F]| + \mathrm{Im}(F)$ is positive definite, and the ranges of $G : X \to Y$ and $F_\sharp^{1/2} : Y \to Y$ coincide.

Making use of lemma 4.10, we can characterize the region beneath the periodic scattering surface in terms of the spectrum of the near-field operators N_j, $j = 1, 2, 3$.

Theorem 4.11. *Let the assumption (**A**) hold and define the sequences $\{C_{p,n}(z)\}_{n\in\mathbb{Z}}$, $\{C_{s,n}(z)\}_{n\in\mathbb{Z}}$ as in (4.2) for $z \in \mathbb{R}^2_\pi$. Then, the point $z \in \mathbb{R}^2_\pi\backslash\overline{\Omega}_\Lambda$ if and only if one of the following conditions holds:*

(i) $\{C_{p,n}(z)\}_{n\in\mathbb{Z}} \in \mathcal{R}\big[(N_{1\sharp})^{1/2}\big]$,
(ii) $\{C_{s,n}(z)\}_{n\in\mathbb{Z}} \in \mathcal{R}\big[(N_{2\sharp})^{1/2}\big]$,
(iii) $\{C_{p,n}(z)\}_{n\in\mathbb{Z}} \times \{C_{s,n}(z)\}_{n\in\mathbb{Z}} \in \mathcal{R}\big[(N_{3\sharp})^{1/2}\big]$,

where $N_{j\sharp} := |\mathrm{Re}[\exp(\mathrm{i}t)N_j]| + \mathrm{Im}(N_j)$, $j = 1, 2, 3$.

Proof. By lemma 4.4, it suffices to verify the coincidence of the ranges of $(N_{j\sharp})^{1/2}$ and G_j for $j = 1, 2, 3$. To do this, we shall apply lemma 4.10 to the factorizations $N_j = -G_j\mathcal{S}_D^*G_j^*$ by verifying the conditions (a)–(d) with $T = -\mathcal{S}_D^*$, $F = N_j$ and $G = G_j$ for $j = 1, 2, 3$. The condition (a) follows from lemma 4.9, while the conditions (c) and (d) follow from lemma 4.7 (iv) and (iii), respectively. It remains to verify the condition (b). Indeed, letting $\omega_1 \in (0, \omega_0]$ and $\phi \in (0, \pi/2)$ be given as in lemma 4.7, we obtain

$$-\mathrm{Re}\langle\varphi, \exp(\mathrm{i}t)\mathcal{S}^{(\omega_1)^*}\varphi\rangle = -\mathrm{Re}\langle\exp(-\mathrm{i}t)\mathcal{S}^{(\omega_1)}\varphi, \varphi\rangle = \mathrm{Re}\langle\varphi, \exp(-\mathrm{i}(t-\pi))\mathcal{S}^{(\omega_1)}\varphi\rangle \tag{4.11}$$

for all $\varphi \in H_\alpha^{-1/2}(\Lambda)^2$. Taking $t = \pi + \phi \in (\pi, 3/2\pi)$ in (4.11), we then conclude from (4.3) and the previous identity that

$$-\mathrm{Re}\langle\varphi, \exp(\mathrm{i}t)\mathcal{S}^{(\omega_1)^*}\varphi\rangle \geqslant c\|\varphi\|^2_{H_\alpha^{-1/2}(\Lambda)^2}, \quad c > 0.$$

This, together with lemma 4.7 (ii), implies the condition (b) in lemma 4.10 with $T_0 = -\mathrm{Re}[\exp(it)\mathcal{S}^{(\omega_1)*}]$ and $T_1 = -\mathrm{Re}[\exp(it)(\mathcal{S}^{(\omega)} - \mathcal{S}^{(\omega_1)})^*]$. □

Let $(\sigma_n^{(j)}, \mathbf{e}_n^{(j)})$ be the eigensystem of $N_{j\sharp}$. By theorem 4.11 and Picard's range criterion [26, theorem A.54], it follows that $z \in \mathbb{R}^2_\pi \backslash \overline{\Omega}_\Lambda$ if and only if one of the following conditions holds:

(i) $\sum_{n=1}^{\infty} |\langle \{C_{p,n}(z)\}_{n\in\mathbb{Z}}, \{\mathbf{e}_n^{(1)}\}_{n\in\mathbb{Z}}\rangle_{l^2}|^2/\sigma_n^{(1)} < \infty$ or, equivalently,

$$W_1(z) = \left[\sum_{n=1}^{\infty} \left|\left\langle \{C_{p,n}(z)\}_{n\in\mathbb{Z}}, \left\{\mathbf{e}_n^{(1)}\right\}_{n\in\mathbb{Z}}\right\rangle_{l^2}\right|^2/\sigma_n^{(1)}\right]^{-1} > 0,$$

(ii) $\sum_{n=1}^{\infty} |\langle \{C_{s,n}(z)\}_{n\in\mathbb{Z}}, \{\mathbf{e}_n^{(2)}\}_{n\in\mathbb{Z}}\rangle_{l^2}|^2/\sigma_n^{(2)} < \infty$ or, equivalently,

$$W_2(z) = \left[\sum_{n=1}^{\infty} \left|\left\langle \{C_{s,n}(z)\}_{n\in\mathbb{Z}}, \left\{\mathbf{e}_n^{(2)}\right\}_{n\in\mathbb{Z}}\right\rangle_{l^2}\right|^2/\sigma_n^{(2)}\right]^{-1} > 0,$$

(iii) $\sum_{n=1}^{\infty} |\langle \{C_{p,n}(z)\}_{n\in\mathbb{Z}} \times \{C_{s,n}(z)\}_{n\in\mathbb{Z}}, \{\mathbf{e}_n^{(3)}\}_{n\in\mathbb{Z}}\rangle_{l^2}|^2/\sigma_n^{(3)} < \infty$ or, equivalently,

$$W_3(z) = \left[\sum_{n=1}^{\infty} \left|\left\langle \{C_{p,n}(z)\}_{n\in\mathbb{Z}} \times \{C_{s,n}(z)\}_{n\in\mathbb{Z}}, \left\{\mathbf{e}_n^{(3)}\right\}_{n\in\mathbb{Z}}\right\rangle_{l^2}\right|^2/\sigma_n^{(3)}\right]^{-1} > 0.$$

Thus, the grating profile Λ can be identified by first selecting sampling points from the set $\{(z_1, z_2) \in \mathbb{R}^2_\pi \ : \ 0 < z_2 < h\}$ and then computing the value of one of the three indicator functions $W_j(z)$, $j = 1, 2, 3$. The values of the indicator function $W_j(z)$ for z lying below the grating profile Λ will be relatively larger than those above the grating profile Λ which are actually zero. In this way, we establish the factorization method in elastic scattering by rigid surfaces, using the $k_p \sin\theta$-quasi-periodic incident elastic waves $u^{\mathrm{in}}_{1,n}$. By the proof of theorem 4.11, the parameter t entering into $N_{j\sharp}$ will be selected depending on the choice of the angle $\phi \in (0, \pi/2)$ given explicitly in the appendix.

Remark 4.12. In inverse acoustic scattering by diffraction gratings, the role of the positive coercive operator is usually played by the single-layer boundary operator whose kernel is the quasi-periodic fundamental solution to the Helmholtz equation with the wavenumber $k = i$ or $k = 0$. This gives rise to an analogous inversion algorithm to theorem 4.11 with the parameter $t = 0$. In the elastic case, more mathematical arguments would be involved in analyzing the Dirichlet-to-Neumann map and the middle operator when $\omega = i$ or $\omega = 0$. This is the reason why we turn to investigate the properties of the middle operator with small frequencies as shown in lemma 4.7 (i). However, our numerical experiments illustrate that the inversion algorithms with $t = 0$ still work well although its theoretical justification is not available yet.

The factorization method using $k_s \sin\theta$-quasi-periodic incident plane waves for the problems $(\mathbf{S}_j)$ can be established analogously.

Corollary 4.13. *Suppose*

(i) ω is not a Dirichlet eigenvalue of the quasi-periodic Lamé operator in the periodic layer Ω_0^- with the phase-shift $\alpha = k_s \sin\theta$,

(ii) either $\sin^2\theta < \mu/(\lambda + 2\mu)$ or $|\sin\theta| > 1/2$ holds.

Then the results of theorem 4.11 for $(\boldsymbol{P}_j)$ apply to the corresponding inverse problems $(\boldsymbol{S}_j)$, $j = 1, 2, 3$.

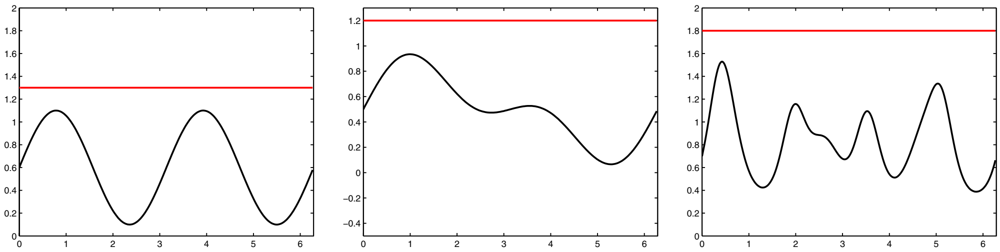

(a) Surface (i) (b) Surface (ii) (c) Surface (iii)

Figure 1. Test surfaces.

Note that the second condition in corollary 4.13 ensures the inequality (4.3) for $\alpha = k_s \sin\theta$; see lemma A.1 (ii). Combining theorem 4.11 and corollary 4.13, we obtain the following uniqueness results by utilizing only the compressional or shear part of the scattered field corresponding to incident elastic waves with a common phase-shift. Define

$$\mathcal{I}(\alpha) := \{(\alpha_n, -\beta_n)^T \exp(\mathrm{i}(\alpha_n x_1 - \beta_n x_2)) : n \in \mathbb{Z}\} \cup \{(\gamma_n, \alpha_n)^T \exp(\mathrm{i}(\alpha_n x_1 - \gamma_n x_2)) : n \in \mathbb{Z}\}$$

Corollary 4.14. *Given an incident angle $\theta \in (-\pi/2, \pi/2)$. Under the conditions in theorem 4.11 (resp. corollary 4.13), a rigid diffraction grating profile can be uniquely determined from the knowledge of the compressional or shear part of the scattered field corresponding to each incoming wave from the set $\mathcal{I}(\alpha)$ with $\alpha = k_p \sin\theta$ (resp. $\alpha = k_s \sin\theta$).*

5. Numerical experiments

In this section, we report numerical experiments to test the validity and accuracy of the factorization method for the inverse problems $(\mathbf{P}_j)$ and $(\mathbf{S}_j)$, $j = 1, 2, 3$. To generate the synthetic scattering data for downward incoming waves $u^{\mathrm{in}}_{j,n,\mathrm{d}}(n \in \mathbb{Z})$ from the set $\mathcal{I}_j(\alpha)$, we solve an equivalent first-kind integral equation on Λ to problem (2.2)–(2.5) by using the discrete Galerkin method given in [13]. The nth Rayleigh coefficients $A^{j,m}_{p,n}$ and $A^{j,m}_{s,n}$ corresponding to the incident wave $u^{\mathrm{in}}_{j,m}$ can be computed through the analysis at the end of section 3. Define the $(2M+1) \times (2M+1)$ matrix $N^{(M)}_{j,\tau}$ as

$$N^{(M)}_{j,\tau} := \begin{pmatrix} A^{j,-M}_{\tau,-M} & A^{j,-M+1}_{\tau,-M} & \cdots & A^{j,0}_{\tau,-M} & \cdots & A^{j,M}_{\tau,-M} \\ A^{j,-M}_{\tau,-M+1} & A^{j,-M+1}_{\tau,-M+1} & \cdots & A^{j,0}_{\tau,-M+1} & \cdots & A^{j,M}_{\tau,-M+1} \\ \vdots & \vdots & \vdots & \vdots & \vdots & \vdots \\ A^{j,-M}_{\tau,M} & A^{j,-M+1}_{\tau,M} & \cdots & A^{j,0}_{\tau,M} & \cdots & A^{j,M}_{\tau,M} \end{pmatrix}, \quad j = 1, 2, \quad \tau = p, s \quad (5.1)$$

for some $M > 0$. Then, the near-field operators N_j $(j = 1, 2)$ can be approximated by the matrices $N^{(M)}_1 := N^{(M)}_{1,p}$ and $N^{(M)}_2 := N^{(M)}_{2,s}$, respectively, whereas the discretization of N_3 leads to the $(4N+2) \times (4N+2)$ matrix

$$N^{(M)}_3 := \begin{pmatrix} N^{(M)}_{1,p} & N^{(M)}_{2,p} \\ N^{(M)}_{1,s} & N^{(M)}_{2,s} \end{pmatrix}.$$

Let the singular value decomposition of $\mathrm{Re}[\mathrm{e}^{\mathrm{i}\phi} N^{(M)}]$ be given by

$$\mathrm{Re}(\mathrm{e}^{\mathrm{i}\phi} N^{(M)}) = VDV^{-1},$$

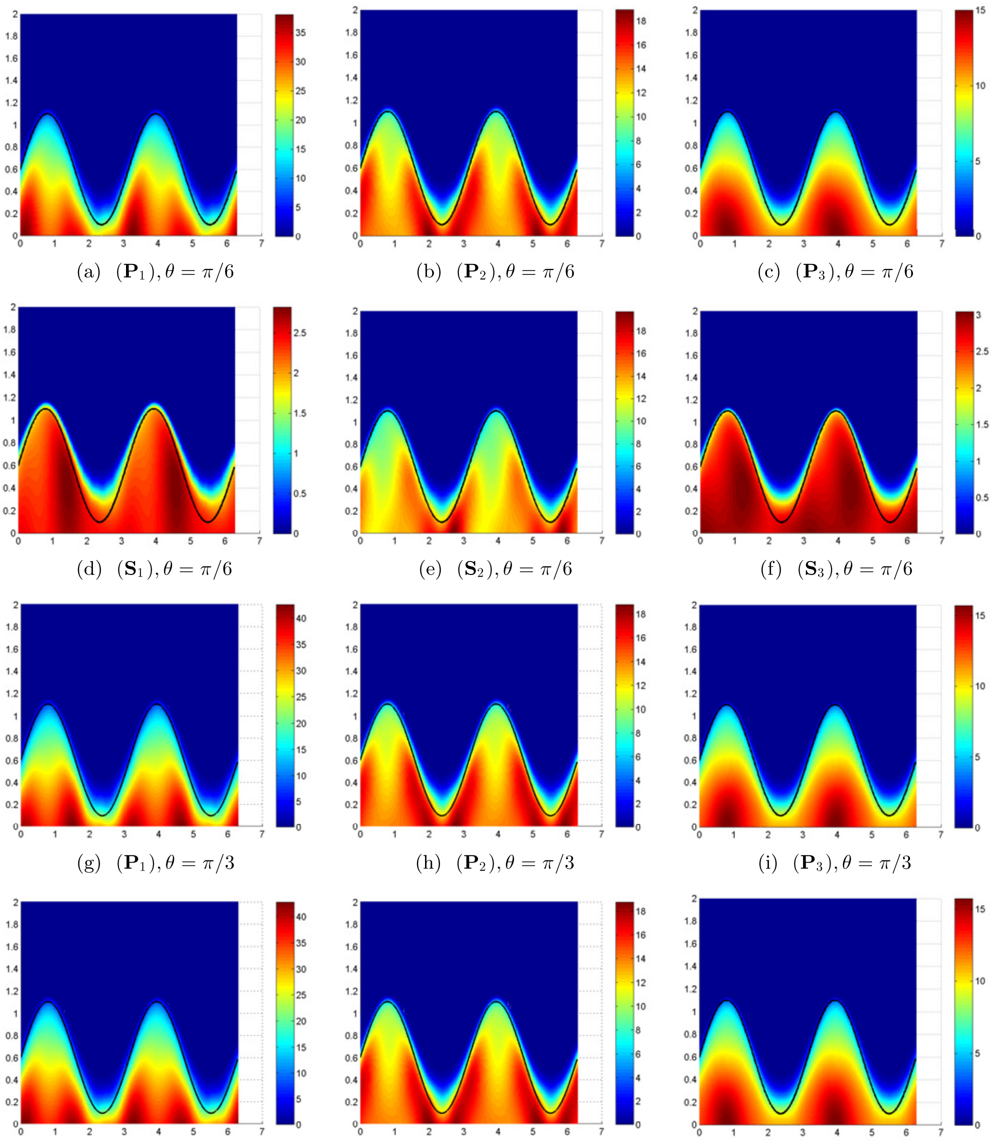

(a) $(\mathbf{P}_1), \theta = \pi/6$ (b) $(\mathbf{P}_2), \theta = \pi/6$ (c) $(\mathbf{P}_3), \theta = \pi/6$

(d) $(\mathbf{S}_1), \theta = \pi/6$ (e) $(\mathbf{S}_2), \theta = \pi/6$ (f) $(\mathbf{S}_3), \theta = \pi/6$

(g) $(\mathbf{P}_1), \theta = \pi/3$ (h) $(\mathbf{P}_2), \theta = \pi/3$ (i) $(\mathbf{P}_3), \theta = \pi/3$

(j) $(\mathbf{S}_1), \theta = \pi/3$ (k) $(\mathbf{S}_2), \theta = \pi/3$ (l) $(\mathbf{S}_3), \theta = \pi/3$

Figure 2. Experiment 1, surface (i): $\omega = 5$, $\lambda = 1$, $\mu = 2$, $M = 30$; $k_p = \sqrt{5}$, $k_s = 5/\sqrt{2}$.

with D being the matrix of eigenvalues and V being the matrix of the corresponding eigenvectors of $\mathrm{Re}(e^{i\phi}N^{(M)})$. Then, the operator $N_\sharp$ can be approximated by

$$N_\sharp^{(M)} = VDV^{-1} + \mathrm{Im}(N^{(M)}).$$

Suppose we have the singular value decomposition of $N_\sharp^{(M)}$:

$$N_\sharp^{(M)} = USU^{-1}$$

with S being the diagonal matrix of singular values σ_l and $U = (\psi_{n,l})$ being the matrix of the left singular vectors. Then, the Picard's range criterion can be approximated by the cut-off series

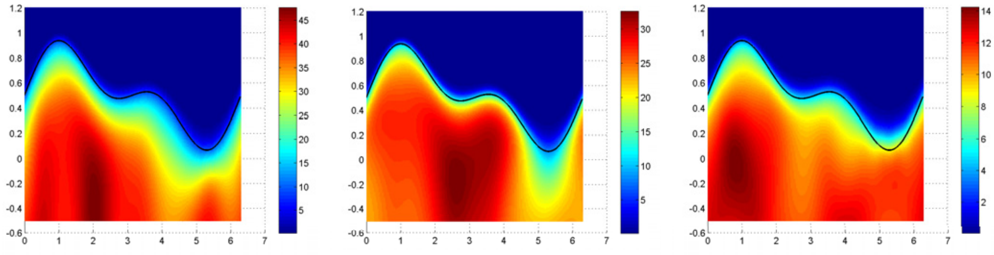

(a) $(\mathbf{P}_1), \theta = \pi/6$ (b) $(\mathbf{P}_2), \theta = \pi/6$ (c) $(\mathbf{P}_3), \theta = \pi/6$

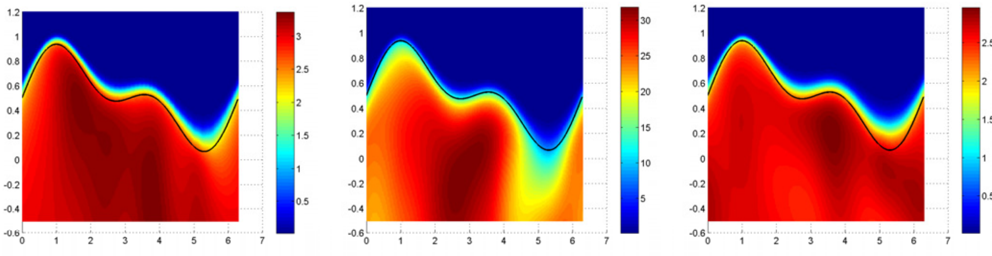

(d) $(\mathbf{S}_1), \theta = \pi/6$ (e) $(\mathbf{S}_2), \theta = \pi/6$ (f) $(\mathbf{S}_3), \theta = \pi/6$

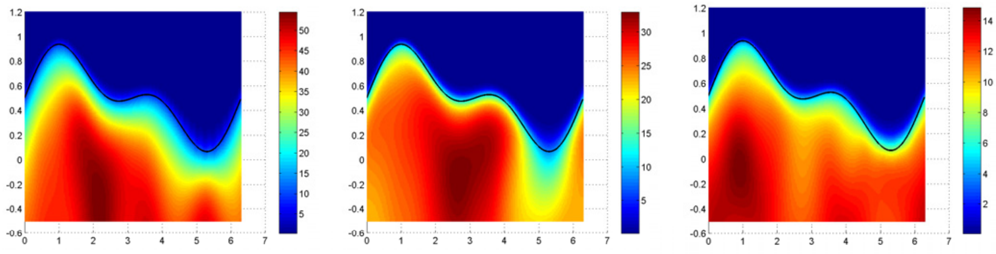

(g) $(\mathbf{P}_1), \theta = \pi/3$ (h) $(\mathbf{P}_2), \theta = \pi/3$ (i) $(\mathbf{P}_3), \theta = \pi/3$

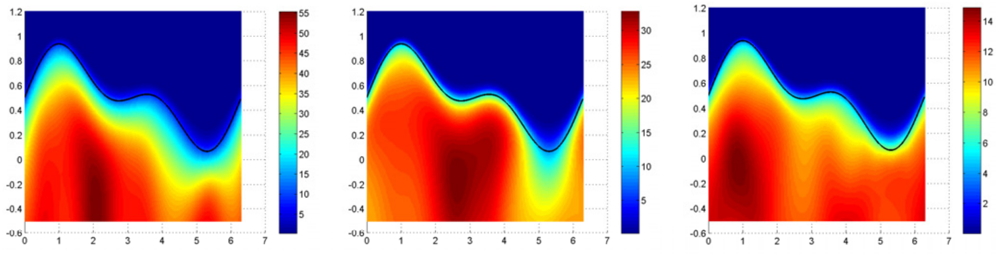

(j) $(\mathbf{S}_1), \theta = \pi/3$ (k) $(\mathbf{S}_2), \theta = \pi/3$ (l) $(\mathbf{S}_3), \theta = \pi/3$

Figure 3. Experiment 1, surface (ii): $\omega = 5$, $\lambda = 1$, $\mu = 2$, $M = 30$; $k_p = \sqrt{5}$, $k_s = 5/\sqrt{2}$.

$$\tilde{W}_1(z) := \left[\sum_{l=1}^{2M+1} \frac{1}{\sigma_l} \left| \sum_{n=-M}^{M} C_{p,n}(z) \overline{\psi}_{n+M+1,l} \right| \right]^{-1},$$

$$\tilde{W}_2(z) := \left[\sum_{l=1}^{2M+1} \frac{1}{\sigma_l} \left| \sum_{n=-M}^{M} C_{s,n}(z) \overline{\psi}_{n+M+1,l} \right| \right]^{-1},$$

$$\tilde{W}_3(z) := \left[\sum_{l=1}^{4M+2} \frac{1}{\sigma_l} \left| \sum_{n=-M}^{M} \left(C_{p,n}(z) \overline{\psi}_{n+M+1,l} + C_{s,n}(z)\right) \overline{\psi}_{n+M+2,l} \right| \right]^{-1}.$$

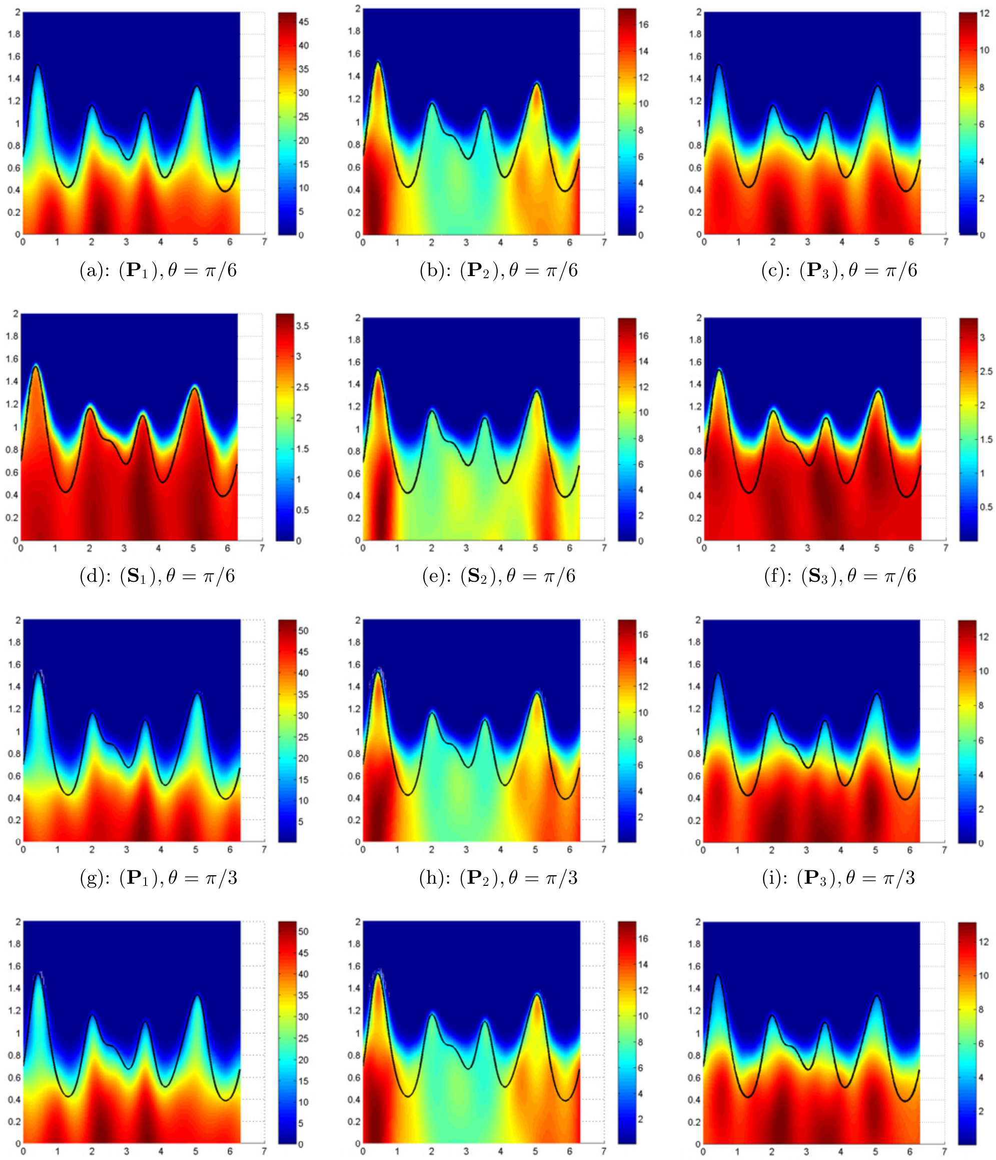

(a): $(\mathbf{P}_1), \theta = \pi/6$ (b): $(\mathbf{P}_2), \theta = \pi/6$ (c): $(\mathbf{P}_3), \theta = \pi/6$

(d): $(\mathbf{S}_1), \theta = \pi/6$ (e): $(\mathbf{S}_2), \theta = \pi/6$ (f): $(\mathbf{S}_3), \theta = \pi/6$

(g): $(\mathbf{P}_1), \theta = \pi/3$ (h): $(\mathbf{P}_2), \theta = \pi/3$ (i): $(\mathbf{P}_3), \theta = \pi/3$

(j): $(\mathbf{S}_1), \theta = \pi/3$ (k): $(\mathbf{S}_2), \theta = \pi/3$ (l): $(\mathbf{S}_3), \theta = \pi/3$

Figure 4. Experiment 1, surface (iii): $\omega = 5, \lambda = 1, \mu = 2, M = 30$; $k_p = \sqrt{5}, k_s = 5/\sqrt{2}$.

We consider the following three grating profiles in our numerical experiments (see figure 1):

(i) $f(x) = 0.6 + 0.5\sin(x), x \in (0, 2\pi), h = 1.3,$
(ii) $f(x) = 0.5 + 0.3\sin(x) + 0.2\sin(2x), x \in (0, 2\pi), h = 1.2,$
(iii) $f(x) = 0.2 + 0.2\exp(\sin(3x)) + 0.3\exp(\sin(4x)), x \in (0, 2\pi), h = 1.8.$

In figure 1, the red horizontal line indicates the detection (or measurement) position Γ_h for the scattered field.

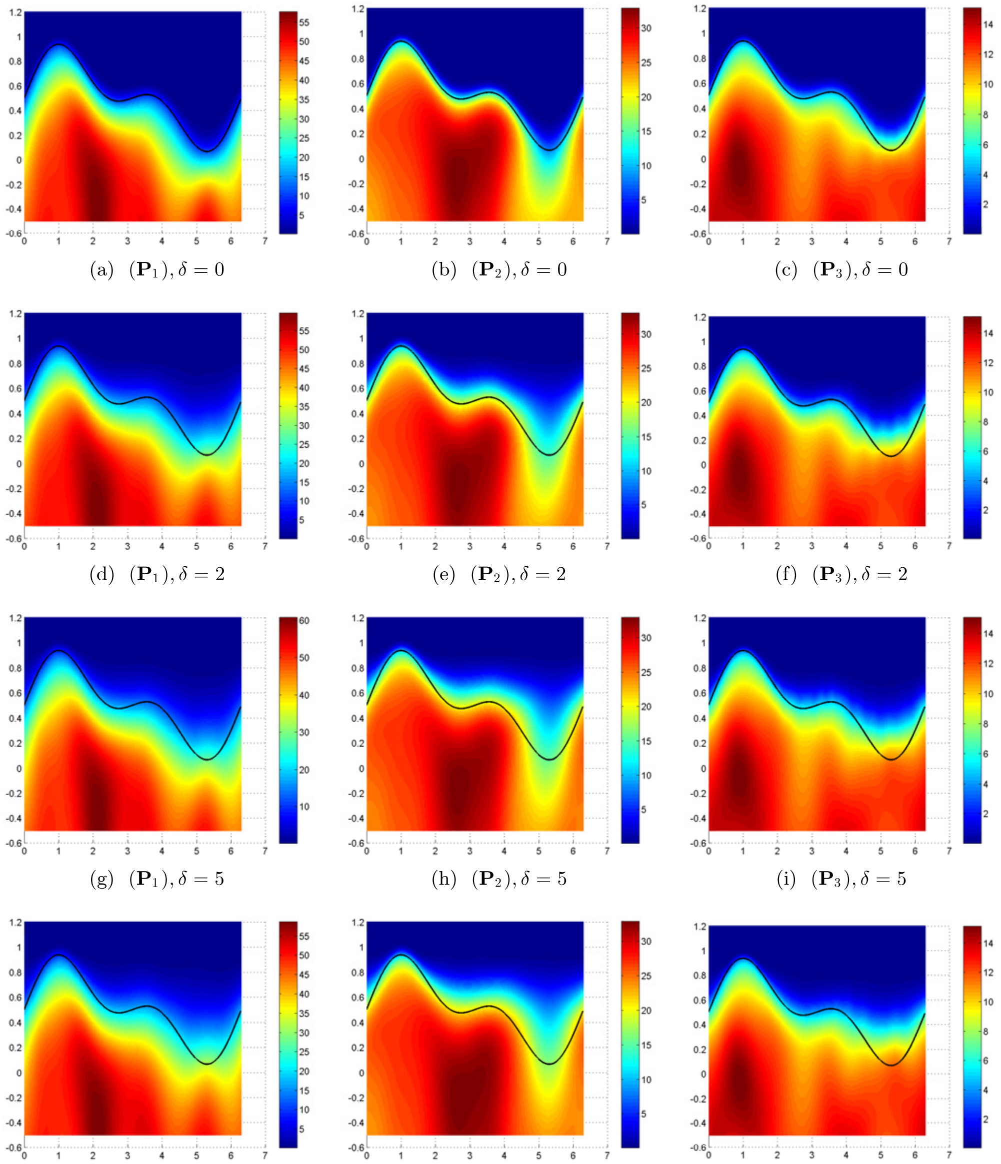

(a) $(\mathbf{P}_1), \delta = 0$ (b) $(\mathbf{P}_2), \delta = 0$ (c) $(\mathbf{P}_3), \delta = 0$

(d) $(\mathbf{P}_1), \delta = 2$ (e) $(\mathbf{P}_2), \delta = 2$ (f) $(\mathbf{P}_3), \delta = 2$

(g) $(\mathbf{P}_1), \delta = 5$ (h) $(\mathbf{P}_2), \delta = 5$ (i) $(\mathbf{P}_3), \delta = 5$

(j) $(\mathbf{P}_1), \delta = 8$ (k) $(\mathbf{P}_2), \delta = 8$ (l) $(\mathbf{P}_3), \delta = 8$

Figure 5. Experiment 2: $\omega = 5, \lambda = 1, \mu = 2, M = 30; k_p = \sqrt{5}, k_s = 5/\sqrt{2}, \theta = 0$.

Experiment 1. We apply the factorization method to the inverse problems $(\mathbf{P}_j)$ and $(\mathbf{S}_j)$, $j = 1, 2, 3$ with fixed parameters $\omega = 5, \lambda = 1, \mu = 2, M = 30$ for distinct incident angles $\theta = \pi/6, \pi/3$. With these settings we have the compressional wavenumber $k_p = \sqrt{5}$ and the shear wavenumber $k_s = 5/\sqrt{2}$, implying that most of our measurement data (Rayleigh coefficients) are from the surface waves with only a few from the propagating modes. We used unpolluted scattered near field taken on Γ_h to reconstruct surfaces (i)–(iii). It can be seen from figures 2–4 that the factorization method gives satisfactory reconstructions particularly for mild surfaces (surface (i)), although poor reconstructions occur when the surface has deep

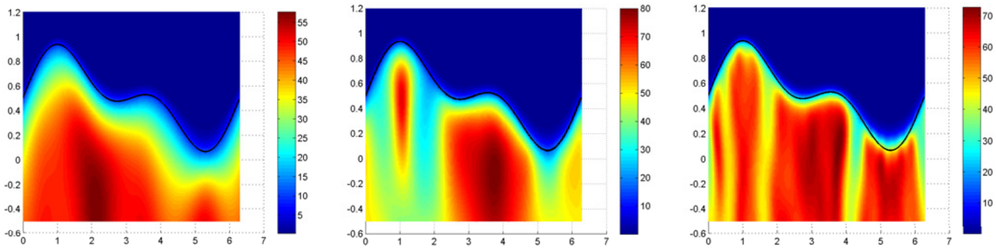

(a) $\omega = 5$ (b) $\omega = 10$ (c) $\omega = 20$

Figure 6. Experiment 3 for different ω, where $\theta = 0$, $M = 30$, $h = 1.2$.

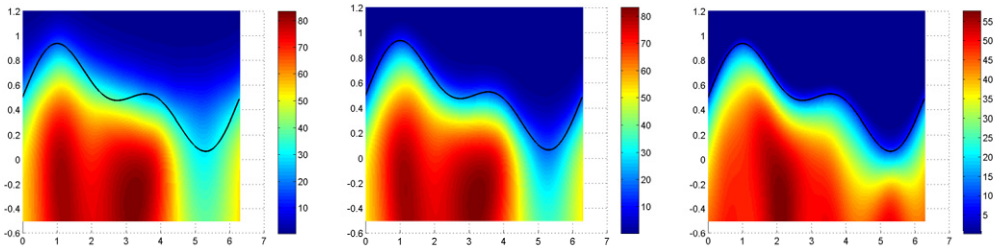

(a) $M = 5$ (b) $M = 15$ (c) $M = 30$

Figure 7. Experiment 3 for different M, where $\omega = 5$, $\theta = 0$, $h = 1.2$.

grooves (e.g., surface (ii)) or oscillates heavily (e.g., surface (iii)). Evidently, using the entire near-field data gives better images than using only P-part or S-part data. In figure 2, the reconstructions for $(\mathbf{P}_j)$ and $(\mathbf{S}_j)$ are nearly the same using different types of incident waves and Rayleigh coefficients, but those for $(\mathbf{P}_3)$ and $(\mathbf{S}_3)$ appear more reliable (see also figures 3 and 4). However, in our settings it is not easy to conclude which one is superior by using P-part data and S-part data. The incident angles seem to have little effect on the quality of the reconstructions.

Experiment 2. We take surface (ii) as an example to investigate the sensitivity of the factorization method to noisy data. We only consider the inverse problems $(\mathbf{P}_j)$, $j = 1, 2, 3$ for the incident angle $\theta = 0$ and take the other parameters as shown in experiment 1. The Rayleigh coefficients are perturbed by the multiplication of $(1 + \delta\%\xi)$ with the noise level $\delta\%$, where ξ is an independent and uniformly distributed random variable generated between -1 and 1. Figure 5 illustrates the reconstructions from different noise levels at $\delta\% = 2\%, 5\%, 8\%$, respectively. It is seen that the factorization method with synthetic data is not very sensitive to the noise, and using the full near-field data seems more stable than using only compressional or shear waves.

Experiment 3. In the final experiment, we want to explore possible approaches to improve the reconstructions. At first, we consider the inverse problem $(\mathbf{P}_1)$ for recovering surface (ii) with fixed $M = 30, \theta = 0$ and with different incidence frequencies $\omega = 5, 10, 20$. Figure 6 shows that higher frequency waves provide more accurate images than using lower frequencies. This can be explained by the fact that the number of propagating modes for $\omega = 20$ ($k_p \approx 8.9$) is much more than that for $\omega = 5$ ($k_p \approx 2.24$). The propagating wave modes contain more information on the scattering surface than the surface (evanescent) modes, because the latter propagates only along the grating profile and decays exponentially in the x_2-direction. This is confirmed again in figure 8 for recovering the surface (iii) with different detection positions. Since surface waves nearly cannot be measured at locations far away from

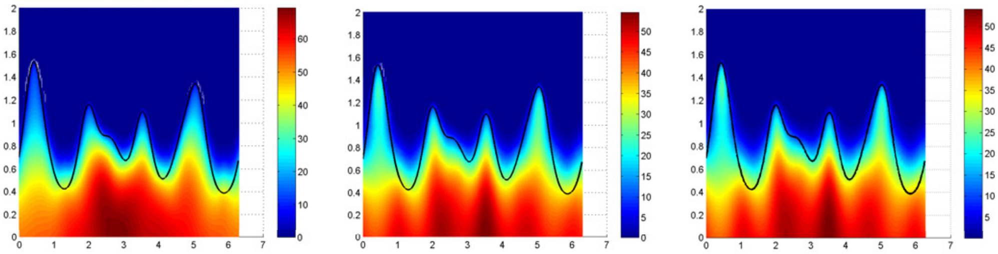

(a) $h = 1.6$ (b) $h = 1.8$ (c) $h = 2.0$

Figure 8. Experiment 3 for different h, where $\omega = 5$, $\theta = 0$, $M = 30$.

the profile, lowering the height of the measurement position contributes to better imaging quality. To see the effects of evanescent waves, we fix $\omega = 5$, $\theta = 0$ and compare the numerical reconstructions of surface (ii) with different M. From figure 7, we conclude that increasing the number of evanescent waves will enhance the imaging quality.

Acknowledgments

The final version of this paper was finished when G Hu visited AMSS, CAS, Beijing in July 2013. The hospitality of the institute is gratefully acknowledged. The first author (GH) is financed by the German Research Foundation (DFG) under grant no. HU 2111/1-1. The work of the third author (BZ) is supported by the National Natural Science Foundation of China under grants 11071243 and 11071244. The authors thank the two reviewers for their constructive comments which helped improve the paper.

Appendix

The following properties of the Dirichlet-to-Neumann (DtN) maps at small frequencies were used in the proof of lemma 4.7 (i). With the help of lemma A.1, we have established the factorization method for any frequency of incidence in section 4.

Lemma A.1.

(i) Let the DtN map $\mathcal{T}_\omega$ *be given by (4.5) with* $\alpha = k_p \sin\theta$*. Then, there exist an angle* $\phi \in (0, \pi/2)$ *and a sufficiently small frequency* $\omega_0 > 0$ *such that*

$$- \operatorname{Re}\left\{\exp(\mathrm{i}\phi)\int_{\Gamma_{\pm h}} \mathcal{T}_\omega u \cdot \bar{u}\, \mathrm{d}s\right\} \geqslant c\,\omega \|u\|^2_{H^{1/2}_\alpha(\Gamma_{\pm h})^2}, \quad c > 0 \tag{A.1}$$

uniformly for $u \in H^{1/2}_\alpha(\Gamma_{\pm h})^2$ *and* $\omega \in (0, \omega_0]$.

(ii) In the case $\alpha = k_s \sin\theta$*, the first assertion remains valid provided either* $\sin^2\theta < \mu/(\lambda + 2\mu)$ *or* $|\sin\theta| > 1/2$.

Proof. (i) We prove (A.1) only for the DtN map defined on Γ_h. By the definition of $\mathcal{T}_\omega$, we have

$$- \int_{\Lambda_h} \mathcal{T}^+_\omega u \cdot \bar{u}\, \mathrm{d}s = \sum_{n\in\mathbb{Z}} (M_{n,\omega} u_n, u_n)_{\mathbb{C}^2}, \qquad \forall u \in H^{1/2}_\alpha(\Gamma_h)^2,$$

where $\{u_n\}_{n\in\mathbb{Z}}$ stands for the Fourier coefficients of $\exp(-\mathrm{i}\alpha x_1) u|_{\Gamma_h}$. Thus, by the definition of the norm of $H^{1/2}_\alpha(\Gamma_{\pm h})^2$ it suffices to prove the existence of $\phi \in (0, \pi/2)$ and $\omega_0 > 0$

such that

$$\mathrm{Re}(\exp(\mathrm{i}\phi)M_{n,\omega}\, z,\ z)_{\mathbb{C}^2} \geqslant c\,\omega\,(1+|n|)\,|z|^2 \quad \text{for all} \quad \omega\in(0,\omega_0],\ n\in\mathbb{Z},\ z\in\mathbb{C}^2. \tag{A.2}$$

Observe that

$$\mathrm{Re}\big(\exp(\mathrm{i}\phi)M_{n,\omega}\big) = \cos\phi\,\mathrm{Re}(M_{n,\omega}) - \sin\phi\,\mathrm{Im}(M_{n,\omega}) \tag{A.3}$$

and that for $\alpha = k_p\sin\theta$,

$$\{n : |\alpha_n| < k_p\} = \{0\},\ \{n : |\alpha_n| > k_s\} = \{n : n \neq 0\},\ \{n : k_p \leqslant |\alpha_n| \leqslant k_s\} = \varnothing \tag{A.4}$$

if $\omega\to 0$. For notational convenience, we write (cf 4.6)

$$M_{n,\omega} = \begin{pmatrix} \mathrm{i}a_n & \mathrm{i}c_n \\ -\mathrm{i}c_n & \mathrm{i}b_n \end{pmatrix}, \quad a_n = \frac{-\omega^2\beta_n}{t_n},\ b_n = \frac{-\omega^2\gamma_n}{t_n},\ c_n = \frac{\alpha_n}{t_n}(\omega^2 - 2\mu t_n). \tag{A.5}$$

We first prove (A.2) in the case $n\neq 0$. Elementary calculation shows that

$$t_n = \alpha_n^2 - \sqrt{\alpha_n^2-k_p^2}\sqrt{\alpha_n^2-k_s^2} = \frac{k_p^2+k_s^2}{2} + \mathcal{O}(\omega^4) \quad \text{as } \omega\to 0. \tag{A.6}$$

Combining (A.4) and (A.6) then yields

$$\begin{aligned} &\mathrm{i}a_n = -\mathrm{i}\omega^2\beta_n/t_n \geqslant c_1\omega(1+|n|) > 0, \quad \mathrm{Im}\,M_{n,\omega} = 0, \\ &\det(\mathrm{Re}\,M_{n,\omega}) = \big(4\alpha_n^2\mu(\omega^2-\mu t_n) - \omega^4\big)/t_n \geqslant c_2\omega^2(1+|n|)^2 > 0 \end{aligned} \tag{A.7}$$

as $\omega\to 0$, with some constants $c_1, c_2 > 0$ independent of u and ω. The estimate (A.2) then follows from (A.7) and (A.3) for all $\phi\in(0,\pi/2)$ and $n\neq 0$.

We next consider the case $n = 0$. In this case, we have $a_0, b_0, c_0, t_0 \in\mathbb{R}$ and

$$\mathrm{Re}(M_{0,\omega}) = \begin{pmatrix} 0 & \mathrm{i}c_0 \\ -\mathrm{i}c_0 & 0 \end{pmatrix}, \quad \mathrm{Im}(M_{0,\omega}) = \begin{pmatrix} a_0 & 0 \\ 0 & b_0 \end{pmatrix}.$$

Consequently,

$$\mathrm{Re}(\exp(\mathrm{i}\phi)M_{0,\omega}) = \begin{pmatrix} -a_0\sin\phi & \mathrm{i}c_0\cos\phi \\ -\mathrm{i}c_0\cos\phi & -b_0\sin\phi \end{pmatrix}.$$

Moreover, the $(1,1)$th entry and the determinant of the above matrix can be more precisely reformulated in terms of λ, μ, ω and ϕ as

$$\begin{aligned} &-a_0\sin\phi = \omega\sqrt{2\mu+\lambda}\cos\theta\sin\phi/H_0(\theta,\lambda,\mu), \\ &\det[\mathrm{Re}(\exp(\mathrm{i}\phi)M_{0,\omega})] = \omega^2(2\mu+\lambda)\big(\tan^2\phi - H_1(\theta,\lambda,\mu)\big)/H_0^2(\theta,\lambda,\mu), \end{aligned}$$

where

$$\begin{aligned} H_0(\theta,\lambda,\mu) &:= \sin^2\theta + \cos\theta\sqrt{(2\mu+\lambda)/\mu - \sin^2\theta} > 0, \\ H_1(\theta,\lambda,\mu) &:= \frac{\sin^2\theta\left[1 - 2\mu\left(\frac{\sin^2\theta}{2\mu+\lambda} + \frac{1}{\sqrt{2\mu+\lambda}}\cos\theta\sqrt{\frac{1}{\mu} - \frac{\sin^2\theta}{2\mu+\lambda}}\right)\right]^2}{\cos\theta\sqrt{(2\mu+\lambda)/\mu - \sin^2\theta}} \geqslant 0. \end{aligned}$$

Taking $\phi\in(0,\pi/2)$ such that $\tan^2\phi > H_1(\theta,\lambda,\mu)$, we obtain

$$-a_0\sin\phi \geqslant c\omega, \quad \det[\mathrm{Re}(\exp(\mathrm{i}\phi)M_{0,\omega})] \geqslant c\omega^2, \quad \forall\omega\in(0,\omega_0]$$

for some constant $c > 0$ independent of $\omega\in(0,\omega_0]$. This yields the estimate (A.2) for $n = 0$. The first assertion is thus proven.

(ii) Let $\alpha = k_s\sin\theta$. If $\sin^2\theta < \mu/(\lambda+2\mu)$ (or equivalently $k_p^2 > k_s^2\sin^2\theta$), then the relations in (A.4) remain valid for small ω. Hence, repeating the same arguments as in proving (i) gives the estimate (A.1) for this case.

Next, consider the case $\sin^2\theta \geqslant \mu/(\lambda+2\mu)$ and $\sin^2\theta > 1/4$. Similarly as in (i), it is enough to prove (A.2).

For $n \neq 0$ and small ω, we have $\beta_n = \mathrm{i}|\beta_n|$, $\gamma_n = \mathrm{i}|\gamma_n|$ and $t_n = \alpha_n^2 - |\beta_n||\gamma_n|$ if $\sin^2\theta \geqslant \mu/(\lambda+2\mu)$. Consequently, by (A.5) we have $\mathrm{Im}(M_{n,\omega}) = 0$ and $(\mathrm{Re}(M_{n,\omega})z, z) \geqslant c\,\omega|n||z|^2$ for $z \in \mathbb{C}^2$, $n \neq 0$, $\omega \in (0, \omega_0]$. Therefore, for any $\phi \in (0, \pi/2)$ one can prove the inequality (A.2) again whenever $n \neq 0$.

Additional arguments are needed in the case $n = 0$, for which we have $\beta_0 = \mathrm{i}|\beta|$, $\gamma_0 = \gamma$, $t_0 = \alpha^2 + \mathrm{i}|\beta|\gamma$ and

$$M_{0,\omega} = \frac{\mathrm{i}}{t_0}N_0, \quad N_0 := \begin{pmatrix} -\mathrm{i}\omega^2\beta & c_0 \\ -c_0 & -\omega^2\gamma \end{pmatrix}, \quad c_0 = \alpha(\omega^2 - 2\mu t_0).$$

By elementary calculations, the matrix $\mathrm{Re}(\mathrm{e}^{\mathrm{i}\phi}M_{0,\omega})$ can be written in the form

$$\mathrm{Re}(\mathrm{e}^{\mathrm{i}\phi}M_{0,\omega}) = \frac{\cos\phi}{\alpha^4 + |\beta|^2\gamma^2}\tilde{N}_{0,\omega},$$
$$\tilde{N}_{0,\omega} := \begin{pmatrix} (\alpha^2 + \tan\phi|\beta|\gamma)\omega^2|\beta| & \mathrm{i}d \\ -\mathrm{i}d & (\tan\phi\alpha^2 - |\beta|\gamma)\omega^2\gamma \end{pmatrix},$$

where

$$d = (\tan\phi\alpha^2 - |\beta|\gamma)2\mu\alpha|\beta|\gamma + (\alpha^2 + \tan\phi|\beta|\gamma)\alpha(\omega^2 - 2\mu\alpha^2).$$

For small ω, the (1, 1)th entry of the matrix $\tilde{N}_{0,\omega}$ has the lower bound

$$(\alpha^2 + \tan\phi|\beta|\gamma)\omega^2|\beta| \geqslant c_1\omega^5, \quad \forall\phi \in (0, \pi/2), \quad c_1 = c_1(\phi) > 0.$$

The determinant of $\tilde{N}_{0,\omega}$ can be written as

$$\det(\tilde{N}_{0,\omega}) = \tan\phi I_1(\theta, \lambda, \mu, \omega) - I_2(\theta, \lambda, \mu, \omega),$$

where

$$I_1 = (\alpha^2 + |\beta|^2\gamma^2)|\beta|\gamma(4\sin^2\theta - 1)\omega^2,$$
$$I_2 = (\alpha^3(\omega^2 - 2\mu\alpha^2) - 2\mu\alpha|\beta|^2\gamma^2)^2 + \omega^4|\beta|^2\gamma^2\alpha^2 > 0.$$

Obviously, $I_1 > 0$ if $|\sin\theta| > 1/2$. Now, choosing $\phi \in (0, \pi/2)$ such that $\tan\phi > I_2/I_1 > 0$, we deduce that

$$\det(\tilde{N}_{0,\omega}) \geqslant c_2\omega^6 \quad \text{as} \quad \omega \to 0$$

for some constant $c_2 = c_2(\phi) > 0$. Finally, making use of the asymptotic behavior $\alpha^4 + |\beta|^2\gamma^2 \sim \omega^4$ as $\omega \to 0$, we obtain (A.2) for $n = 0$ when $\sin^2\theta \geqslant \mu/(\lambda+2\mu)$ and $\sin^2\theta > 1/4$. The second assertion (ii) is thus proved. □

Remark A.2. Note that in the case $|\sin\theta| < 1/2$, we have $\det(\tilde{N}_{0,\omega}) < 0$, and the matrix $\mathrm{Re}(\mathrm{e}^{\mathrm{i}\phi}M_{0,\omega})$ is then not definite.

References

[1] Ammari H 1995 Uniqueness theorems for an inverse problem in a doubly periodic structure *Inverse Problems* **11** 823–33

[2] Antonios C, Drossos G and Kiriakie K 2001 On the uniqueness of the inverse elastic scattering problem for periodic structures *Inverse Problems* **17** 1923–35

[3] Arens T 1999 The scattering of plane elastic waves by a one-dimensional periodic surface *Math. Methods Appl. Sci.* **22** 55–72

[4] Arens T 1999 A new integral equation formulation for the scattering of plane elastic waves by diffraction gratings *J. Integral Eqns Appl.* **11** 275–97

[5] Arens T and Grinberg N 2005 A complete factorization method for scattering by periodic surface *Computing* **75** 111–32

[6] Arens T and Kirsch A 2003 The factorization method in inverse scattering from periodic structures *Inverse Problems* **19** 1195–211

[7] Bao G, Cowsar L and Masters W (ed) 2001 *Mathematical Modeling in Optical Science* (Philadelphia, PA: SIAM)

[8] Bonnet-Bendhia A S and Starling P 1994 Guided waves by electromagnetic gratings and non-uniqueness examples for the diffraction problem *Math. Methods Appl. Sci.* **17** 305–38

[9] Chandler-Wilde S N and Elschner J 2012 Variational apporach in weighted Sobolev spaces to scattering by unbounded rough surfaces *SIAM J. Math. Anal.* **42** 2554–80

[10] Charalambopoulos A, Kirsch A, Anagnostopoulos K A, Gintides D and Kiriaki K 2007 The factorization method in inverse elastic scattering from penetrable bodies *Inverse Problems* **23** 27–51

[11] Elschner J and Hu G 2010 Variational approach to scattering of plane elastic waves by diffraction gratings *Math. Methods Appl. Sci.* **33** 1924–41

[12] Elschner J and Hu G 2012 Scattering of plane elastic waves by three-dimensional diffraction gratings *Math. Models Methods Appl. Sci.* **22** 1150019

[13] Elschner J and Hu G 2012 An optimization method in inverse elastic scattering for one-dimensional grating profiles *Commun. Comput. Phys.* **12** 1434–60

[14] Elschner J and Hu G 2013 Elastic scattering by unbounded rough surfaces: solvability in weighted Sobolev spaces *WIAS Preprint No.* 1780 (Berlin, Germany: Weierstrass Institute)

[15] Elschner J, Hsiao G C and Rathsfeld A 2003 Grating profile reconstruction based on finite elements and optimization techniques *SIAM J. Appl. Math.* **64** 525–45

[16] Fokkema J T 1980 Reflection and transmission of elastic waves by the spatially periodic interface between two solids (theory of the integral-equation method) *Wave Motion* **2** 375–93

[17] Fokkema J T and Van den Berg P M 1977 Elastodynamic diffraction by a periodic rough surface (stress-free boundary) *J. Acoust. Soc. Am.* **62** 1095–101

[18] Hettlich F 2002 Iterative regularization schemes in inverse scattering by periodic structures *Inverse Problems* **18** 701–14

[19] Hettlich F and Kirsch A 1997 Schiffer's theorem in inverse scattering for periodic structures *Inverse Problems* **13** 351–61

[20] Hu G, Kirsch A and Sini M 2013 Some inverse problems arising from elastic scattering by rigid obstacles *Inverse Problems* **29** 015009

[21] Ito K and Reitich F 1999 A high-order perturbation approach to profile reconstruction: I. Perfectly conducting grating *Inverse Problems* **15** 1067–85

[22] Kirsch A 1993 Diffraction by periodic structures *Proc. Lapland Conf. on Inverse Problems* ed L Päivärinta *et al* (Berlin: Springer) pp 87–102

[23] Kirsch A 1998 Characterization of the shape of a scattering obstacle using the spectral data of the far field operator *Inverse Problems* **14** 1489–512

[24] Kirsch A 2004 The factorization method for Maxwell's equations *Inverse Problems* **20** S117–34

[25] Kirsch A and Grinberg N 2008 *The Factorization Method for Inverse Problems* (New York: Oxford University Press)

[26] Kirsch A 2011 *An Introduction to the Mathematical Theory of Inverse Problems* 2nd edn (New York: Springer)

[27] Linton C M 1998 The Green's function for the two-dimensional Helmholtz equation in periodic domains *J. Eng. Math.* **33** 377–401

[28] Lechleiter A 2008 Factorization methods for photonics and rough surfaces *PhD Thesis* University of Karlsruhe, Karlsruhe, Germany

[29] Nakagawa S, Nihei K T, Myer L R and Majer E L 2003 Three-dimensional elastic wave scattering by a layer containing vertical periodic fractures *J. Acoust. Soc. Am.* **113** 3012–23

[30] Nguyen D L 2012 Spectral methods for direct and inverse scattering from periodic structures *PhD Thesis* Ecole Polytechnique, Palaiseau, France

[31] Sandfort K 2010 The factorization method for inverse scattering from periodic inhomogeneous media *PhD Thesis* University of Karlsruhe, Karlsruhe, Germany

[32] Turunen J and Wyrowski F (ed) 1997 *Diffractive Optics for Industrial and Commercial Applications* (Berlin: Akademie)

[33] Yang J, Zhang B and Zhang R 2012 A sampling method for the inverse transmission problem for periodic media *Inverse Problems* **28** 035004

[34] Yang J, Zhang B and Zhang R 2013 Reconstruction of penetrable grating profiles *Inverse Problems Imaging* at press